UNIVERSITY OF CALIFORNIA

SANTA CRUZ

Cks and Speedy Confer Specificity to Cyclin-dependent kinase

A dissertation submitted in partial satisfaction

of the requirements for the degree of

DOCTOR OF PHILOSOPHY

in

CHEMISTRY & BIOCHEMISTRY

by

Denise Ann McGrath

September 2016

The Dissertation of Denise Ann McGrath

is approved:

_____

Professor Seth Rubin

_____

Professor Doug Kellogg

_____

Professor Carrie Partch

_____

Tyrus Miller

Vice Provost and Dean of Graduate Studies

Table of Contents

Page

List of Figures

List of Tables

Table **Page**

Abstract

Denise Ann McGrath

Cks and Speedy Confer Specificity to Cyclin-dependent kinase

Inappropriate cell division and aberrant cell cycles are the hallmarks of cancer. Cyclin dependent kinases (CDKs) are the master regulators of the cell cycle. CDK activity drives cells to divide and suppression of CDK activity inhibits cell division. It is crucial to understand mechanisms of CDK regulation, as many cancers are correlated with inactivating mutations to CDK inhibitors and upregulation of CDK activators. This dissertation presents research that utilizes X-ray crystallography, kinetic assays, and various biochemical and biophysical methods to examine two different aspects of CDK regulation. The first aspect focuses on the small protein called Cyclin-dependent kinases regulatory subunit (Cks). We've shown that Cks confers specificity to CDK toward substrates via a phosphate-binding pocket. This specificity is required for multi-site phosphorylation of these substrates as well as *in vivo* viability. The second aspect investigates the mechanism of CDK activation by the atypical cyclin-like protein Speedy A. Using kinetic assays and X-ray crystallography we have elucidated the molecular source of CDK activation by Speedy. The structure shown shows how Speedy is a potent CDK activator whose expression overrides normal inhibitory cell cycle signaling. These findings reveal the molecular source of CDK regulation by Cks and Spy1 proteins and can inform the development of these proteins as prognostic markers for cancers and design of design of cancer therapeutics.

Chapter 1: Introduction to CDK Regulation

Cell division is the means by which all life grows and reproduces. Eukaryotic cells must coordinate the replication and partitioning of cellular contents in preparation for cell division. These events, termed the cell cycle, happen in strict temporal order to ensure fidelity of cell replication. Problems in maintaining the order of events in the cell cycle lead to cell instability, cell death, and cancer.[1] Consequently, the molecular mechanisms that ensure ordered cell cycle events are of great research interest.

Many of the of the molecules involved in the cell cycle progression have been well-studied and cell cycle investigators have a deep understanding of the events of cell division. Over the long history of cell cycle research, some key events and molecular players have emerged. The transition from G1 to S is irreversible and marks the point at which the cell becomes committed to cell division. Given the importance to cells in preventing inappropriate cell division, the molecular mechanisms of regulation of this transition are of great interest to research. Passing the G1-S checkpoint requires convergence of a multitude of extra-cellular and intracellular signals on the regulation of Retinoblastoma protein (Rb) and the SCF complex. Another key phase transition is located at the entry to mitosis and is gated by the activity of Wee1 kinase and Cdc25 phosphatase. The last key phase transition is at the entry of anaphase, when the chromosome copies separate in preparation of the final stages of cell division. Anaphase entry is controlled by the activity of the anaphase-promoting complex (APC). While hundreds of proteins participate in the events that lead to cell division. It has long been recognized that Cyclin-dependent kinase (CDK) is the driving force behind progression through the eukaryotic cell cycle.[2]

Inappropriate CDK activation is recognized to be a feature common to many cancers. Much of CDK activity is regulated by the abundance of Cyclin proteins and their overexpression contributes to tumorigenesis.[3, 4] Cyclin D and E overexpression cause unregulated transition from G1 to S phase[5, 6], committing cells to the cell cycle in the absence of the correct mitogenic signals. Overexpression of Cyclins A and B, which promote transition through later

phases of the cell cycle, are correlated with genomic instability and poor prognosis in many cancers.[7-9] Endogenous CDK inhibitor proteins (CKIs) such as the INK4 and Cip/Kip families oppose the action of Cyclins. Timely expression and degradation of CKIs contribute to the cell's ordered progression through the cell cycle. Downreguation and mutations that inhibit function are implicated in multiple cancer types.[10-13]

CDKs are proline-directed serine/threonine protein kinases that catalyze the transfer of the γ-phosphate from ATP to the side-chain oxygen of a serine or a threonine. Hundreds of CDK substrates have been discovered using proteomic screens, and phosphorylation of these substrates alters their structure, interaction, localization, and stability.[14, 15] CDKs prefer to phosphorylate an optimal consensus sequence of S/T-P-X-K/R.[16] CDK is well conserved in all eukaryotes, with simple organisms like yeast possessing only one homolog while complex organisms like humans possessing upwards of 10 different homologs. In humans, many of the CDKs have evolved to fill specialized roles in specific tissues. The mammalian cell cycle requires four different CDKs for passage through the checkpoints. These CDK are highly similar with just over 30% sequence identity. The remainder of this dissertation focuses on the regulation of human CDK1 and 2 and I will refer to them as simply "CDK". In most cases the two kinases are interchangeable as they share 64% sequence identity. The CDK monomer is inactive and requires association with an activation subunit and phosphorylation for full activity. Early studies of CDK activation portray the states of individual CDK molecules in a binary fashion: either fully inhibited or fully active.[17, 18] But recent studies, including the contents of this dissertation, are shedding light on roles for gradations of specificity and activity of CDK molecules in the cell cycle.

At the primary level of regulation, CDK is activated and inhibited by a core of four mechanisms. The primary and essential activation mechanism occurs though Cyclin protein binding. Cyclins confer a structural change to the CDK, which properly positions catalytic residues in the active site and allows CDK to bind ATP. Rapid production and subsequent degradation of specific Cyclins at each cell cycle stage confers activity and specificity to CDK.

The specificity conferred by Cyclins stems from a docking interaction between a conserved hydrophobic patch on the Cyclins and an RXL amino acid motif that is C-terminus to the phosphorylation site on the substrate.[19, 20] It is thought that this is one mechanism by which CDK can target its cell-cycle stage-specific substrates among the multitude of possible substrates and produce the temporally-ordered molecular events of the cell cycle.

The CDK/Cylin complex is only partially active, showing 100-fold less kinase activity than the fully active complex. In the second mechanism of CDK regulation, a loop of the CDK sequence that blocks the active site (the aptly-named T-loop) is phosphorylated on T160 by CDK-activating kinase (CAK). Unphosphorylated, the T-loop occludes the active site and prevents efficient binding of peptide substrates, resulting in low CDK activity. Phosphorylation by CAK causes the T-loop to be drawn out of the active site so that it can bind substrate peptides and results in a 100-fold increase in enzyme activity. It is this binary combination of Cyclin-binding and T-loop phosphorylation that produces what is considered the fully-active CDK.

The last two mechanisms of CDK regulation are inhibitory. CDKs are phosphorylated on conserved residues T14 and Y15 by Myt1 and Wee1 kinases, respectively. Phospho-T14 inhibits phosphate transfer and phospho-Y15 inhibits ATP binding. The kinases and phosphatase (Cdc25) responsible for adding and removing these phosphates are themselves phosphorylated by CDK. This feedback loop is an interesting example of apparent self-regulation by CDK, the mechanisms of which are explored by many researchers. [21-23]

Lastly, CDKs are also inhibited by association with a family of proteins called the Cyclin-dependent kinases inhibitors (CKIs). The INK4 family of inhibitors allosterically prevent cyclin and ATP binding to CDK. The Cip/Kip family of proteins bind to the CDK/Cyclin complex that is phosphorylated on the T-loop and not on Y15. They associate with the cyclins through their RXL-binding motif, make contacts with CDK that distort the catalytic site, and insert a 3_{10} helix into the active site to competitively inhibit ATP binding. Both families of inhibitors are targeted for degradation when phosphorylated by CDK: another example of CDK seemingly

participating in self-regulation.

It is thought that preceding a checkpoint, the majority of CDK-Cyclin complexes are inhibited, but poised for activity. The convergence of the correct signals results in the rapid removal of the inhibitory phosphates, phosphorylation of the T-loop, and degradation of the CKIs, thereby flipping the switch from a pool of inactive CDK to a pool of fully-active CDK. It has been shown that the self-regulating behavior of CDK at multiple points in the cell cycle can be explained by a threshold model of CDK activity. In this model, as cyclin levels increase, a small pool of either partially active or fully-active CDK phosphorylates its own regulators, thereby increasing the pool of fully-active CDK. This then creates a feed-back loop that results in cell-wide CDK activity quickly reaching the threshold required for initiating the events require to pass cell cycle checkpoints.

Though the core CDK regulatory mechanisms and models are well-tested and accepted, there remain many proteins of unknown function that directly interact with and regulate CDK activity and modulate the cell cycle. This dissertation contains my contribution and the contribution of other like-minded researchers to the study of these CDK-regulating proteins.

In the second chapter I will describe the results of biochemical and biophysical characterization of the Cyclin-dependent kinases regulatory subunit (Cks). Cks binds to CDK distal to the Cyclin-binding interface and enhances multisite phosphorylation of cell cycle regulatory proteins.[24, 25] Cks' role in the cell cycle is not well understood and it's upregulation is correlated with poor prognosis in cancer.[26-29] This dissertation contains the results of a publication which elucidate the molecular details of CKs specificity and it's role in multisite phosphorylation.[30]

The third chapter contains the results of biophysical studies of a non-canonical cyclin-like protein Speedy A. Speedy replaces Cyclin to activate CDK, it's overexpression enhances cell proliferation, and is implicated in hepatocellular carcinoma, lymphoma, malignant glioma, ovarian cancer, and breast cancer.[31-35] The studies contained in this dissertation portray Speedy as potent CDK activator that bypasses canonical CDK regulation.

References

1. Sherr, C. J., Cancer cell cycles. *Science* **1996,** *274* (5293), 1672-7.

2. Morgan, D. O., Principles of CDK regulation. *Nature* **1995,** *374* (6518), 131-4.

3. Hartwell, L. H.; Weinert, T. A., Checkpoints: controls that ensure the order of cell cycle events. *Science* **1989,** *246* (4930), 629-34.

4. Hartwell, L. H.; Kastan, M. B., Cell cycle control and cancer. *Science* **1994,** *266* (5192), 1821-8.

5. Bates, S.; Peters, G., Cyclin D1 as a cellular proto-oncogene. *Semin Cancer Biol* **1995,** *6* (2), 73-82.

6. Sandhu, C.; Slingerland, J., Deregulation of the cell cycle in cancer. *Cancer Detect Prev* **2000,** *24* (2), 107-18.

7. Tane, S.; Chibazakura, T., Cyclin A overexpression induces chromosomal double-strand breaks in mammalian cells. *Cell Cycle* **2009,** *8* (23), 3900-3.

8. Baldini, E.; Camerini, A.; Sgambato, A.; Prochilo, T.; Capodanno, A.; Pasqualetti, F.; Orlandini, C.; Resta, L.; Bevilacqua, G.; Collecchi, P., Cyclin A and E2F1 overexpression correlate with reduced disease-free survival in node-negative breast cancer patients. *Anticancer Res* **2006,** *26* (6B), 4415-21.

9. Nar, A.; Ozen, O.; Tutuncu, N. B.; Demirhan, B., Cyclin A and cyclin B1 overexpression in differentiated thyroid carcinoma. *Med Oncol* **2012,** *29* (1), 294-300.

10. Harper, J. W., Cyclin dependent kinase inhibitors. *Cancer Surv* **1997,** *29*, 91-107.

11. Lee, J.; Kim, S. S., The function of p27 KIP1 during tumor development. *Exp Mol Med* **2009,** *41* (11), 765-71.

12. Drexler, H. G., Review of alterations of the cyclin-dependent kinase inhibitor INK4 family genes p15, p16, p18 and p19 in human leukemia-lymphoma cells. *Leukemia* **1998,** *12* (6), 845-59.

13. Dome, J. S.; Look, A. T., Three molecular determinants of malignant conversion and their potential as therapeutic targets. *Curr Opin Oncol* **1999,** *11* (1), 58-67.

14. Holt, L. J.; Tuch, B. B.; Villen, J.; Johnson, A. D.; Gygi, S. P.; Morgan, D. O., Global analysis of Cdk1 substrate phosphorylation sites provides insights into evolution. *Science* **2009,** *325* (5948), 1682-6.

15. Ubersax, J. A.; Woodbury, E. L.; Quang, P. N.; Paraz, M.; Blethrow, J. D.; Shah, K.; Shokat, K. M.; Morgan, D. O., Targets of the cyclin-dependent kinase Cdk1. *Nature* **2003,** *425* (6960), 859-64.

16. Loog, M.; Morgan, D. O., Cyclin specificity in the phosphorylation of cyclin-dependent kinase substrates. *Nature* **2005,** *434* (7029), 104-8.

17. Marcote, M. J.; Pagano, M.; Draetta, G., cdc2 protein kinase: structure-function relationships. *Ciba Found Symp* **1992,** *170*, 30-41; discussion 41-9.

18. Pines, J., Protein kinases and cell cycle control. *Semin Cell Biol* **1994,** *5* (6), 399-408.

19. Schulman, B. A.; Lindstrom, D. L.; Harlow, E., Substrate recruitment to cyclin-dependent kinase 2 by a multipurpose docking site on cyclin A. *Proc Natl Acad Sci U S A* **1998,** *95* (18), 10453-8.

20. Koivomagi, M.; Valk, E.; Venta, R.; Iofik, A.; Lepiku, M.; Morgan, D. O.; Loog, M., Dynamics of Cdk1 substrate specificity during the cell cycle. *Mol Cell* **2011,** *42* (5), 610-23.

21. Harvey, S. L.; Charlet, A.; Haas, W.; Gygi, S. P.; Kellogg, D. R., Cdk1-dependent regulation of the mitotic inhibitor Wee1. *Cell* **2005,** *122* (3), 407-20.

22. Harvey, S. L.; Enciso, G.; Dephoure, N.; Gygi, S. P.; Gunawardena, J.; Kellogg, D. R., A phosphatase threshold sets the level of Cdk1 activity in early mitosis in budding yeast. *Mol Biol Cell* **2011,** *22* (19), 3595-608.

23. Perry, J. A.; Kornbluth, S., Cdc25 and Wee1: analogous opposites? *Cell Div* **2007,** *2*, 12.

24. Bourne, Y.; Watson, M. H.; Hickey, M. J.; Holmes, W.; Rocque, W.; Reed, S. I.; Tainer, J. A., Crystal structure and mutational analysis of the human CDK2 kinase complex with cell cycle-regulatory protein CksHs1. *Cell* **1996,** *84* (6), 863-74.

25. Patra, D.; Wang, S. X.; Kumagai, A.; Dunphy, W. G., The xenopus Suc1/Cks protein promotes the phosphorylation of G(2)/M regulators. *J Biol Chem* **1999,** *274* (52), 36839-42.

26. Pines, J., Cell cycle: reaching for a role for the Cks proteins. *Curr Biol* **1996,** *6* (11), 1399-402.

27. Lan, Y.; Zhang, Y.; Wang, J.; Lin, C.; Ittmann, M. M.; Wang, F., Aberrant expression of Cks1 and Cks2 contributes to prostate tumorigenesis by promoting proliferation and inhibiting programmed cell death. *Int J Cancer* **2008,** *123* (3), 543-51.

28. Liberal, V.; Martinsson-Ahlzen, H. S.; Liberal, J.; Spruck, C. H.; Widschwendter, M.; McGowan, C. H.; Reed, S. I., Cyclin-dependent kinase subunit (Cks) 1 or Cks2 overexpression overrides the DNA damage response barrier triggered by activated oncoproteins. *Proc Natl Acad Sci U S A* **2012,** *109* (8), 2754-9.

29. Shen, D. Y.; Fang, Z. X.; You, P.; Liu, P. G.; Wang, F.; Huang, C. L.; Yao, X. B.; Chen, Z. X.; Zhang, Z. Y., Clinical significance and expression of cyclin kinase subunits 1 and 2 in hepatocellular carcinoma. *Liver Int* **2010,** *30* (1), 119-25.

30. McGrath, D.; Balog, E. R. M.; Kõivomägi, M.; Lucena, R.; Mai, M. V.; Hirschi, A.; Kellogg, D. R.; Loog, M.; Rubin, S. M., Cks Confers Specificity to Phosphorylation-Dependent Cdk Signaling Pathways In Revision at Nature Structural and Molecular Biology, 2013.

31. Porter, L. A.; Dellinger, R. W.; Tynan, J. A.; Barnes, E. A.; Kong, M.; Lenormand, J. L.; Donoghue, D. J., Human Speedy: a novel cell cycle regulator that enhances proliferation through activation of Cdk2. *J Cell Biol* **2002,** *157* (3), 357-66.

32. Lu, S.; Liu, R.; Su, M.; Wei, Y.; Yang, S.; He, S.; Wang, X.; Qiang, F.; Chen, C.; Zhao, S.; Zhang, W.; Xu, P.; Mao, G., Spy1 participates in the proliferation and apoptosis of epithelial ovarian cancer. *J Mol Histol* **2016,** *47* (1), 47-57.

33. Hang, Q.; Fei, M.; Hou, S.; Ni, Q.; Lu, C.; Zhang, G.; Gong, P.; Guan, C.; Huang, X.; He, S., Expression of Spy1 protein in human non-Hodgkin's lymphomas is correlated with phosphorylation of p27 Kip1 on Thr187 and cell proliferation. *Med Oncol* **2012,** *29* (5), 3504-14.

34. Ke, Q.; Ji, J.; Cheng, C.; Zhang, Y.; Lu, M.; Wang, Y.; Zhang, L.; Li, P.; Cui, X.; Chen, L.; He, S.; Shen, A., Expression and prognostic role of Spy1 as a novel cell cycle protein in hepatocellular carcinoma. *Exp Mol Pathol* **2009,** *87* (3), 167-72.

35. Zhang, L.; Shen, A.; Ke, Q.; Zhao, W.; Yan, M.; Cheng, C., Spy1 is frequently overexpressed in malignant gliomas and critically regulates the proliferation of glioma cells. *J Mol Neurosci* **2012,** *47* (3), 485-94.

Chapter 2: Cks Confers Specificity to Phosphorylation-Dependent CDK Signaling Pathways

Introduction

Many Cdk substrates contain multiple phosphorylation sites. The mechanism of targeting specific proteins for multisite phosphorylation by Cdk has not been well-studied. It is critical to understand the role of multisite phosphorylation in the cell cycle as dysregulation of protein phosphorylation is correlated with cancer.[1] Cyclin-dependent kinase regulatory subunit (Cks).is a protein known to promote Cdk-dependent multisite phosphorylation of cell -cycle regulators[2], but the function of Cks has been a mystery to cell cycle researchers for decades.[3] Understanding the functional and mechanistic details of Cks is important as Cks upregulation has been correlated with poor prognosis in caner.[4-6]

Early structures of Cks show that it binds to Cdk on a surface that is opposite of the Cyclin-binding interface, indicating that Cdk can bind both Cyclin and Cks simultaneously. Also, Cks has been crystallized with either phosphate or vanadate in a conserved pocket of positively-charged residues that is distal to the Cdk2 active site.[7, 8] These observations have led to a model in which Cks binds to Cdk substrates that have been primed by phosphorylation. (Fig. 2.1) This binding would act as a docking interaction which increases Cdk's affinity for these phospho-primed substrates and allow for efficient multisite phosphorylation. It was recently found that multisite phosphorylation of the G1/S regulator, Sic1, relies on an intact Cks anion-binding pocket[9], but it was not known whether Cks binds

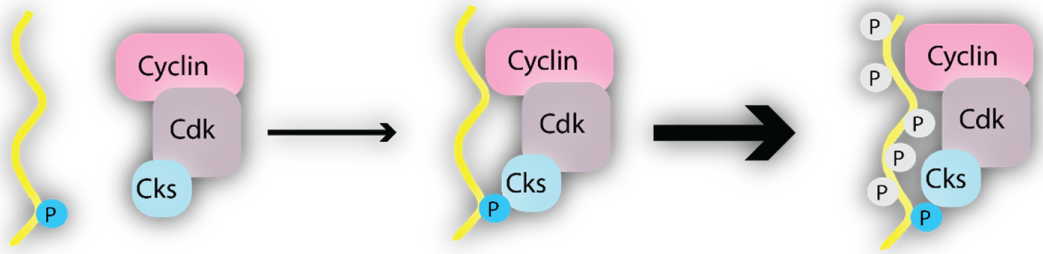

Figure 2.1 The priming model of multisite phosphorylation Cks has been hypothesized to bind Cdk substrates that are primed by phosphorylation, thereby increasing the affinity of the kinase complex for it's substrates, conferring specificity toward primed substrates, and enhancing multisite phosphorylation.

any phosphosite or if there were additional specificity requirements. The result that follow show that Cks associates with specific phosphosites and elucidate the molecular mechanism of Cks specificity.

Results

Cks binds to specific phosphorylated sites in Cdk substrates

A number of phosphorylation-dependent Cdk-substrate complexes have been reported[22,38], and we and others have demonstrated that Cks binds to phosphorylated sequences in intrinsically disordered domains of several Cdk substrates[24,39]. To test whether Cks binds specific phosphorylated sites, we examined the affinity of *S. cerevisiae* Cks (Cks1) for the N -terminal domain of the replication-licensing factor Cdc6. As determined by isothermal titration calorimetry (ITC), Cks1 binds to phosphorylated $Cdc6^{1-48}$ with K_d = 9.8 ± 0.2 μM, while no detectable heat was measured for the unphosphorylated protein (Figure 2.1a). The presence of two distinct and independent Cks1 binding sites in $phosCdc6^{1-48}$ is supported by the stoichiometry parameter; the data fit to a one site model with n » 2, indicating that two molecules of Cks1 bind noncooperatively to each phosphorylated Cdc6 molecule.

We then mutated different combinations of phosphoacceptor sites and found that Cks1 binds to $Cdc6^{1-48}$ phosphorylated only at T7 and T23 ($Cdc6^{1-48;T39A\ S43A}$) with a similar affinity and stoichiometry as fully phosphorylated $Cdc6^{1-48}$ (Figure 2.2b and Appendix Figure A1). In contrast, no detectable binding signal was observed with $Cdc6^{1-48}$ phosphorylated only at T39 and S43. Cdc6 constructs in which only T7 ($Cdc6^{1-48;T23A\ T39A\ S43A}$) or T23 ($Cdc6^{1-48;T7A\ T39A\ S43A}$) are phosphorylated bind with similar affinity as the wild-type protein but have stoichiometries n » 1. We also tested binding of Cks1 to synthetic peptides, $phosCdc^{2-10}$ and $phosCdc6^{19-26}$, which only contain phosphorylated T7 or T23 respectively. Each bound to Cks1 with an affinity about 10-fold less than phosphorylated Cdc^{1-48}. A $Cdc6^{1-48}$ construct in which T7 and T23 are mutated to alanine and the sequence surrounding T39 is replaced with the T7 sequence

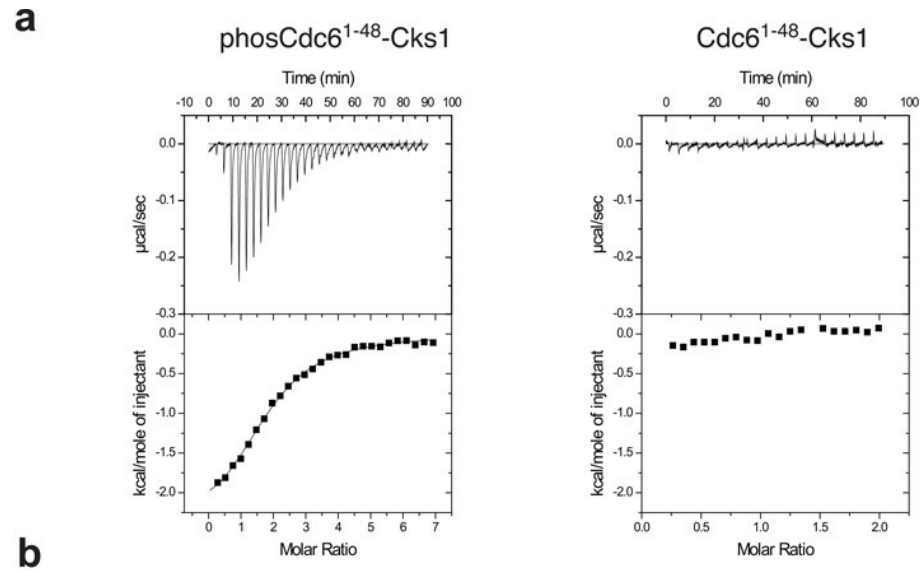

b

		Cks1 K_d (ITC)	Molar ratio
phosCdc6$^{1-48}$	MSAIPITPTKRIRRNLFDDAPATPPRPLKRKKLQFTDVTPESSPEKLQ	9.8 ± 0.2 µM	1.8 ± 0.1
Cdc6$^{1-48}$	MSAIPITPTKRIRRNLFDDAPATPPRPLKRKKLQFTDVTPESSPEKLQ	No binding	—
phosCdc6$^{1-48;T39A\ S43A}$	MSAIPITPTKRIRRNLFDDAPATPPRPLKRKKLQFTDVAPESAPEKLQ	8 ± 2 µM	2.0 ± 0.2
phosCdc6$^{1-48;T7A\ T23A}$	MSAIPIAPTKRIRRNLFDDAPAAPPRPLKRKKLQFTDVTPESSPEKLQ	No binding	—
phosCdc6$^{1-48;T23A\ T39A\ S43A}$	MSAIPITPTKRIRRNLFDDAPAAPPRPLKRKKLQFTDVAPESAPEKLQ	12 ± 2 µM	0.9 ± 0.2
phosCdc6$^{1-48;T7A\ T39A\ S43A}$	MSAIPIAPTKRIRRNLFDDAPATPPRPLKRKKLQFTDVAPESAPEKLQ	11 ± 3 µM	1.0 ± 0.1
phosCdc6$^{2-10}$	SAIPITPTK	130 ± 60 µM	1.00 ± 0.01
phosCdc6$^{19-26}$	APATPPR	140 ± 30 µM	1.03 ± 0.01
phosCdc6$^{1-48;T7-T39swap}$	MSAIPIAPTKRIRRNLFDDAPAAPPRPLKRKKLQAIPITPTKSPEKLQ	17 ± 6 µM	1.2 ± 0.1

Figure 2.2 Cks1 binds specific phosphorylated Cdk sites in the N-terminal domain of Cdc6. (a) Purified Cdc61–48 was phosphorylated with recombinant Cdk and affinity for Cks1 was measured by isothermal titration calorimetry. phosCdc61–48 binds Cks1 with Kd = 9.8 ± 0.2 µM (fit of data on left), while titration of unphosphorylated Cdc61–48 does not yield any binding heat (right). (b) ITC measurements with phosphorylated Cdc61–48 constructs and synthetic peptides demonstrate that two sites, T7 and T23, are each sufficient for Cks binding. Sequence mutations are highlighted in red within each construct. ITC data curves not shown in part (a) are shown in Appendix Figure A1A–A1G

(Cdc6$^{1-48;T7-T39swap}$) binds Cks1 with wild-type affinity. We conclude that the majority of the cohesive interactions are contained within short sequences including the phosphothreonines and suggest that the peptides bind with slightly lower affinity due to a greater entropy penalty. Together these data demonstrate that T7 or T23 phosphorylation is necessary and sufficient for Cks1 association and that Cks1 has binding requirements beyond the minimum phosphorylated (S/T)P Cdk site.

We tested the minimum sequence around T7 required for binding Cks1 using a dot-blot assay. Synthetic phosphopeptides were cross-linked to BSA, spotted onto a PVDF membrane, and the membrane was then incubated with His-tagged Cks1 and probed with an anti-His antibody (Figure 2.3a). We found that the 7-mers AIPIpTPT and IPIpTPTK peptide were sufficient for Cks1 binding. ITC measurements confirmed that AIPI(pT)P, SAIPI (pT)P, and AIPI(pT)PT bind Cks1 with similar affinity as phosCdc6$^{2-10}$ (Table 1). We substituted phosphoserine and phosphotyrosine for phosphothreonine and observed no binding to Cks1 in both the dot-blot and ITC assays.

In order to identify the Cdc6 sequence determinants of Cks affinity, we used SPOT arrays with peptides directly synthesized on a membrane (Figure 2.3b). Every spot contains a version of the phosCdc6$^{3-10}$ sequence in which a single substitution is made at each position with each of the twenty amino acids. The array was probed as described above, except Cks1 was alkylated to prevent the formation of disulfide linkages (Figure 2.4). We observed that no residue is tolerated at the pT position (0 position), including the phosphomimetics glutamate and aspartate, and that proline is required in the +1 position. This result indicates that all Cks1 binding sequences contain the phosphorylated Cdk consensus site TP. Cks1 also displays a marked propensity for binding to peptides with a bulky hydrophobic residue in the -2 position. The array demonstrates that any residue is tolerated in the -4, -3, +2, and +3 positions, although a basic residue or proline seems to be disfavored in the +2 position. There appears to be a varied preference in the -1 position, however there is no clear correlation between the chemical properties of the tolerated sidechains.

In order to corroborate that these observations are general for Cks1 binding and are not influenced by subtle effects of the specific Cdc6$^{3-10}$ sequence context, we conducted the array based on a sequence in Sic1 (Figure 2.3c). Sic1 T5 is a preferred Cdk phosphorylation site that serves as a priming site for Cks-dependent phosphorylation[24].

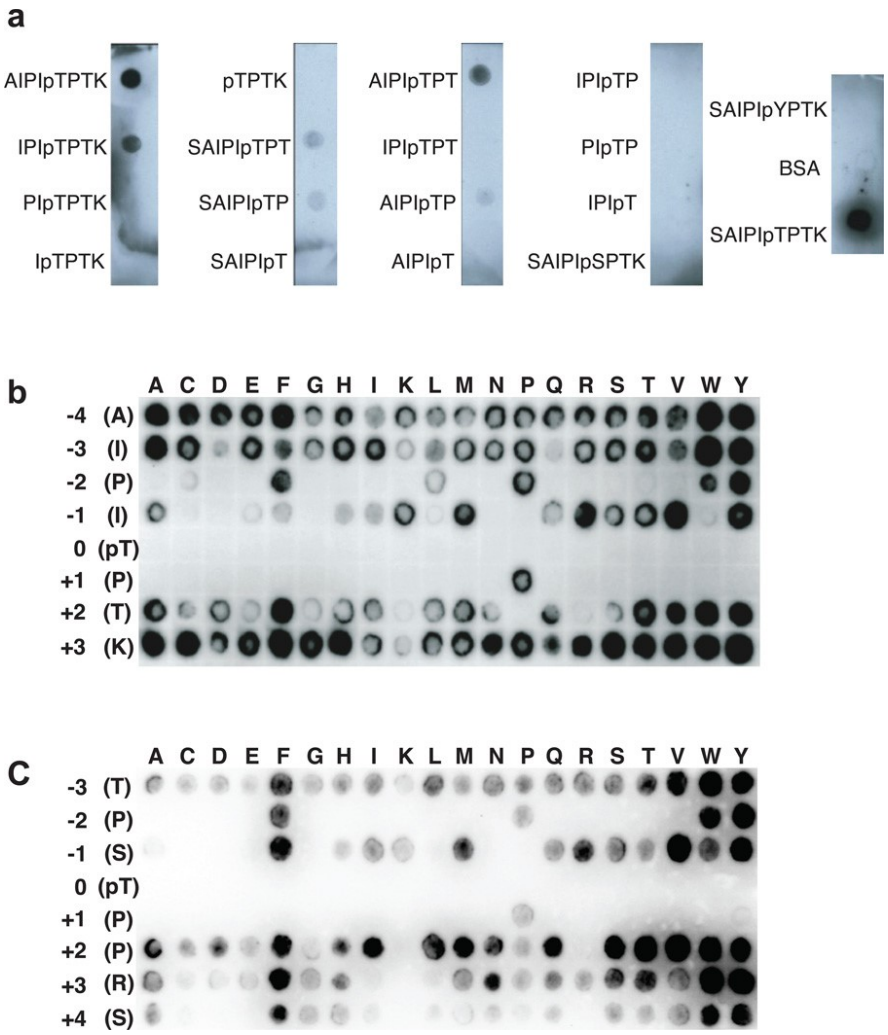

Figure 2.3 Sequence requirements for Cks1 binding. (a) Dot-blot peptide experiment to determine the minimum length required for association with Cks1. The indicated peptides were conjugated to BSA, spotted onto PVDF membrane, incubated with His-tagged Cks1, and probed with an anti-His antibody. The data demonstrate the requirement of a 7-mer containing a phosphothreonine. (b) Scanning mutagenesis SPOT peptide array based on the Cdc6$^{3-10}$ AIPIpTPTK peptide. Peptides containing the indicated single-amino acid substitution were synthesized onto the membrane and probed for Cks1 binding as in (a). (c) Similar to (b), except the array is constructed from a phosphorylated Sic1$^{2-9}$ peptide. (Eva Balog)

Probing a phosSic1$^{2-9}$ array for Cks1 binding, we again found a requirement for phosphothreonine and proline in the 0 and +1 positions respectively, a preference for a bulky hydrophobic residue in the -2 position, and a disfavoring of a positive residue in the +2 position.

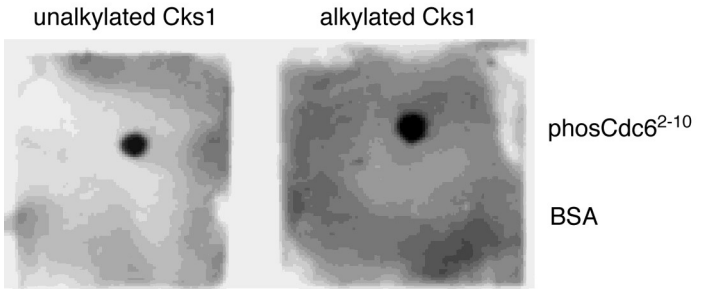

Figure 2.4 Alkylation of Cks1 does not abrogate binding of phosphopeptides. The wild-type phosCdc6$^{2-9}$ peptide was probed with Cks1 and alkylated Cks1 as described for Figure 2a. Alkylation, which was confirmed by mass spectrometry, occurs on a single cysteine that is distal to the phosphate-binding pocket.

We performed ITC with Cks1 and phosCdc6$^{2-10}$ peptides to confirm and quantify the spot array results (Table 1). Replacing the phosphothreonine for a different phosphorylated sidechain (pT7pS and pT7pY) or substitution of the +1 proline (P8K) results in loss of detectable heat. Substitutions of aromatic residues for the proline in the -2 position have little effect or slightly increase binding affinity relative to wild-type, whereas substitution of a charged lysine at the -2 position (P5K) results in no detectable heat. The +2 position in the SPOT array disfavored a positive charge or proline. However, by ITC, we found that substitution of a proline (T9P) or a lysine (T9K) for the +2 threonine results in a binding affinity similar to wild-type peptide.

Three Cdk sites (T5, T33, and T45) in the Sic N-terminal domain (Sic1$^{1-215}$, "Sic1DC") facilitate Cks binding, and these sites are known to promote priming-dependent phosphorylation[24]. T5 and T45 contain a proline in the -2 position and their phosphorylation promotes higher affinity binding to Cks than T33, which contains a glutamate in the -2 position (data not shown). We measured affinity for wild-type and substituted phosSic1$^{2-9}$ peptides (Table 1 and Appendix Figure A1). PhosSic1$^{2-9}$ binds with a slightly weaker affinity (K_d = 95 ± 8 mM) than the entire phosphorylated Sic1 N-terminus and phosSic1DC that only contains T5 as a phosphoacceptor site (K_d = 11±3mM and K_d = 20 ± 10 mM respectively[24]).

Table 2.1. Binding affinities of Cks1 to phosphorylated Cdk substrate peptides

Peptide	Sequence	Cks1 K_d (μM)	Supplemental Figure
phosCdc6$^{2-10}$	SAIPI(pT)PTK	130 ± 60	1E
phosCdc6$^{19-26}$	APAp(T)PPR	140 ± 30	1F
phosCdc6$^{3-8}$	AIPI(pT)P	81 ± 6	1H
phosCdc6$^{2-8}$	SAIPI(pT)P	62 ± 2	1I
phosCdc6$^{3-9}$	AIPI(pT)PT	61 ± 9	1J
phosCdc6$^{2-10; pT7pS}$	SAIPI(pS)PTK	no heat	1K
phosCdc6$^{2-10; pT7pY}$	SAIPI(pY)PTK	no heat	1L
phosCdc6$^{2-10; P8K}$	AIPI(pT)KTK	no heat	1M
phosCdc6$^{2-10; P5Y}$	AIYI(pT)PTK	190 ± 1	1N
phosCdc6$^{2-10; P5F}$	AIFI(pT)PTK	50 ± 30	1O
phosCdc6$^{2-10; P5K}$	AIKI(pT)PTK	no heat	1P
phosCdc6$^{2-10; T9P}$	AIPI(pT)PPK	129 ± 8	1Q
phosCdc6$^{2-10; T9K}$	AIPI(pT)PKK	158 ± 4	1R
phosSic1$^{2-9}$	TPS(pT)PPRS	95 ± 8	1S
phosSic1$^{2-9; pT5pS}$	TPS(pS)PPRS	no heat	1T
phosSic1$^{2-9; P6K}$	TPS(pT)KPRS	no heat	1U
phosSic1$^{2-9; P3Y}$	TYS(pT)PPRS	90 ± 50	1V
phosSic1$^{2-9; P3K}$	TKS(pT)PPRS	no heat	1W
phosSic1$^{2-9; P7T}$	TPS(pT)PTRS	70 ± 20	1X
phosSic1$^{2-9; P7K}$	TPS(pT)PKRS	120 ± 20	1Y
phosSwe1$^{41-48}$	IGGS(pT)PTN	no heat	1GG
phosSwe1$^{117-124}$	ESVT(pT)PIT	170 ± 90	1HH
phosSwe1$^{192-199}$	RIPE(pT)PVK	60 ± 10	1II
phosSwe1$^{369-376}$	EEIS(pT)PTR	160 ± 70	1JJ

As in the case of Cdc6, this observation suggests an interaction between the immediate sequence surrounding T5 and Cks1. The affinities of phosSic1$^{2-9}$ peptides with single amino acid substitutions show the same trend as Cdc6 peptides (Table 1). The ITC measurements are also consistent with the SPOT array data, with the exception that a positive lysine is tolerated in the +2 position in the ITC measurements.

Structural basis of Cks binding specificity

We next determined the 2.9 Å crystal structure of a Cks1-phosCdc6 complex to understand the molecular determinants of the specificity observed in our binding experiments (Table 2

and Figure 2.5). Crystals were grown using a fusion protein construct, phosphorylated after purification, in which the Cdc6$^{3-9}$ sequence was appended to the C-terminus of Cks1$^{1-112}$ (Appendix Figure A2). The Cdc6 sequence binds across a surface of Cks1 that is distal to the Cdk binding site and made up of one face of the Cks1 b-sheet and helix 2 (Figure 2.5a). The phosphate on the Cdc6 T7 sidechain is bound to the previously described cationic pocket (Figure 2.5b)[33,34]. The Cdc6 T7 γ-methyl makes van der Waals contacts with Y30 and R42 in Cks1, which explains the specificity for phosphothreonine over phosphoserine. Cdc6 P8, which is in the +1 position, fits into a pocket formed by both Y30 and T80 in Cks1. The fact that no other hydrophobic residues are tolerated in this +1 position suggests that geometry constraints in the Cdc6 backbone are important for proline specificity. The

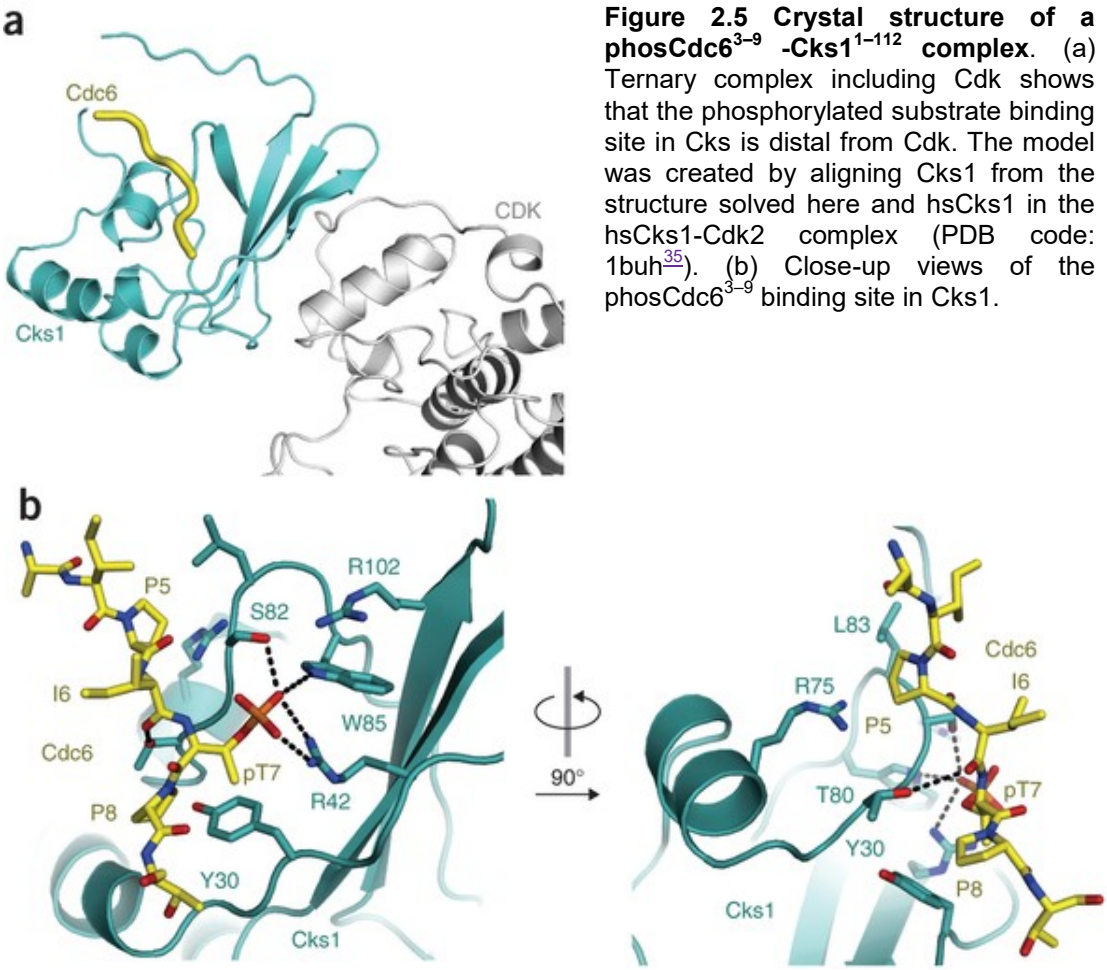

Figure 2.5 Crystal structure of a phosCdc6$^{3–9}$ -Cks1$^{1–112}$ complex. (a) Ternary complex including Cdk shows that the phosphorylated substrate binding site in Cks is distal from Cdk. The model was created by aligning Cks1 from the structure solved here and hsCks1 in the hsCks1-Cdk2 complex (PDB code: 1buh[35]). (b) Close-up views of the phosCdc6$^{3–9}$ binding site in Cks1.

dihedral angles adopted by the +1 proline (phi = ~-80, psi = ~-160) to contact Y30 and T80 are relatively disfavored by other residues. The loss of affinity upon proline substitution likely arises from the compromise of maintaining the sidechain-Cks1 contacts and adopting

Table 2.2 Data collection and refinement statistics

	phosCdc6$^{3-9}$ -Cks1$^{1-112}$
Data collection	
Space group	$P4_12_12$
Cell dimensions	
a, *b*, *c* (Å)	84.7, 84.7, 239.9
α, β, γ (°)	90, 90, 90
Resolution (Å)	60.0-2.9 (3.06-2.90)
R_{merge}	0.0463 (0.2598)
$I / \sigma I$	12.65 (3.57)
Completeness (%)	99.79 (99.90)
Redundancy	10.0 (9.9)
Refinement	
Resolution (Å)	58.1-2.9
No. reflections	20,140
R_{work} / R_{free}	24.5% / 28.1%
No. atoms	3852
Protein	3800
Ligand/ion	0
Water	52
B factors	56.5 Å^2
Protein	47.60
Ligand/ion	n/a
Water	52.30
r.m.s. deviations	
Bond lengths (Å)	0.011
Bond angles (°)	1.39

One crystal was used. *Values in parentheses are for highest-resolution shell.

such strained torsion angles. The γ-hydroxyl of Cks1 T80 acts as a hydrogen bond donor to the backbone carbonyl of I6 (-1 position) in Cdc6. Although there is no clear correlation among the chemical properties of the tolerated amino acids at the -1 position in the array data (Figure 2.5b and 2.5c), this hydrogen bond may select for particular backbone dihedral preferences that best facilitate its formation.

A second pocket formed by Cks L83 and R75 fits Cdc6 P5 (the -2 position). The distances to the -2 proline sidechain explain the preference for a large hydrophobic residue in this position. The presence of R75, which is highly conserved in Cks proteins, is also consistent with the observed preference for aromatic residues in the -2 position of the binding consensus (Figure 2.5b and 2.5c), as the guanidinium group is capable of making cation-pi interactions with aromatic sidechains[40]. There are few interactions in the crystal structure between Cks1 and residues in the +2, +3, and -3 positions in the Cdc6 peptide, which is consistent with our observation that any amino acid type can substitute there.

The importance of the molecular interactions observed in the crystal structure of the Cks1-phosCdc6 complex were verified with single amino acid mutations to Cks1. Y30E, R75A, R75K, T80D, and L83D Cks1 mutants were purified and tested for binding to phosCdc6 by ITC. The structure shows that Y30 and T80 are important for binding the +1 proline, while R75 and L83 form the pocket to accommodate the -2 proline. All the mutants were folded properly, as determined by circular dichroism (Appendix Figure 3a). As predicted by the structure, mutations at these positions inhibited binding to the phosCdc6$^{2-10}$ peptide in the calorimetry assay; in each case, no heat was detected (Appendix Figure A1Z-A1DD).

Priming-dependent Cdk phosphorylation requires Cks-substrate binding

We next explored the implications of Cks-substrate docking for its function in stimulating Cdk activity towards cell cycle substrates. We previously found that priming phosphorylation of Sic1 facilitates semiprocessive phosphorylation of critical phosphodegrons, and the requirement for an intact Cks1 cationic pocket demonstrated the importance of Cks-dependent kinetics for Cdk signaling[24]. The structural details of the Cks-

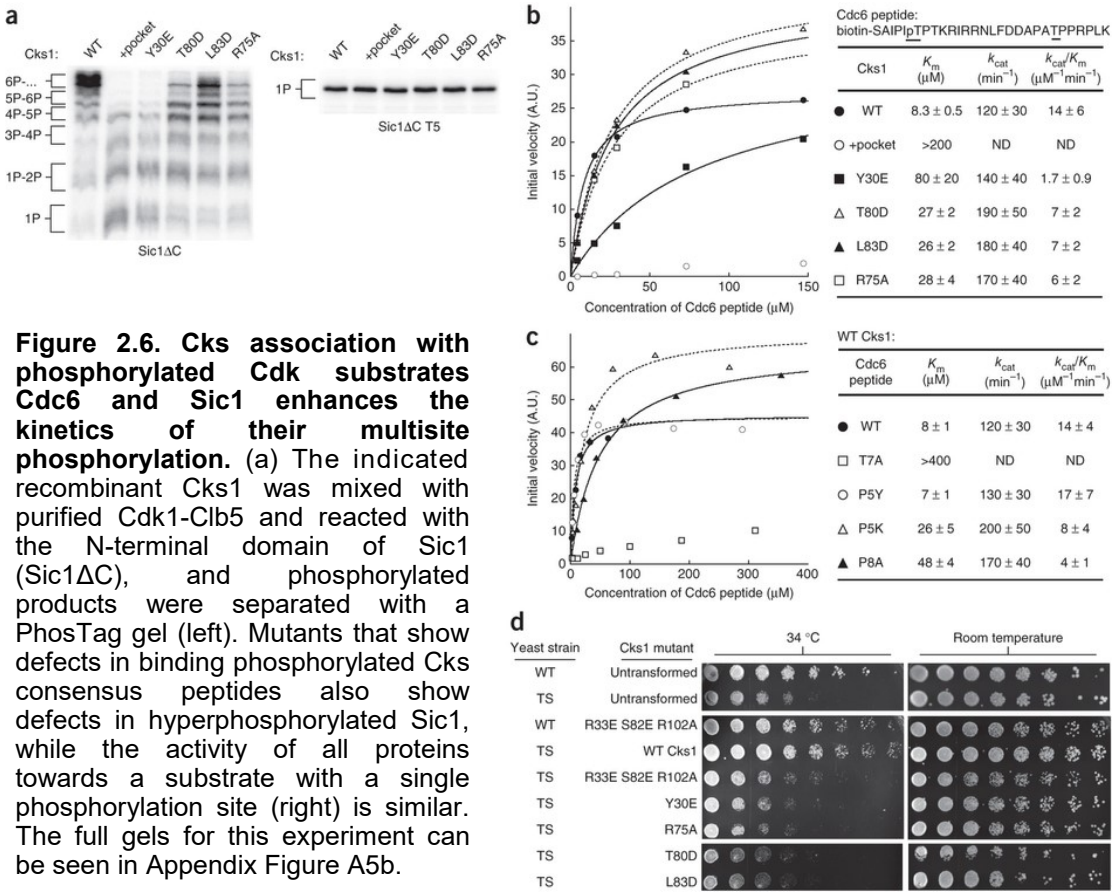

Figure 2.6. Cks association with phosphorylated Cdk substrates Cdc6 and Sic1 enhances the kinetics of their multisite phosphorylation. (a) The indicated recombinant Cks1 was mixed with purified Cdk1-Clb5 and reacted with the N-terminal domain of Sic1 (Sic1ΔC), and phosphorylated products were separated with a PhosTag gel (left). Mutants that show defects in binding phosphorylated Cks consensus peptides also show defects in hyperphosphorylated Sic1, while the activity of all proteins towards a substrate with a single phosphorylation site (right) is similar. The full gels for this experiment can be seen in Appendix Figure A5b.

(b) Steady-state kinetics of Cdk1-Clb5 mixed with wild-type and mutant Cks1 proteins. The substrate is a synthetic Cdc6 peptide that contains a priming Cks consensus phosphate (phosT7) and an additional phosphoacceptor site (T23). (c) As in (b) except that wild-type Cks1 is used in each experiment with the indicated Cdc6 peptide mutation. (d) Cks1 mutants defective in consensus binding cannot rescue temperature-sensitive Cks1-mutant budding yeast. Temperature sensitive (TS) and wild-type (WT) strains were transformed with a CEN vector containing either wild-type yeast Cks1 or a Cks1 point mutant, grown in selective media to saturation, plated at 1:5 serial dilutions, and grown again at room temperature or 34°C.(a-c: Mardo Kõivomägi)

substrate complex observed here allowed us to test specifically the effect of disrupting this complex on Cdk kinetics. We tested whether Cks1 mutations that abolish interactions with substrate residues inhibit multisite phosphorylation (Figure 2.6). As previously described[24], recombinant Cks1 was added to Cdk1-Clb5 purified from budding yeast, and the enzyme was used to phosphorylate the non-inhibitory truncation Sic1ΔC in a kinase assay. In the reaction with wild-type Cks1, hyperphosphorylated species are present within 8 minutes and

are the dominant product (Figure 2.6a). Previous substrate competition experiments established that the rapid accumulation of these hyperphosphorylated forms is due to a semiprocessive mechanism[24]. In contrast, hyperphosphorylated Sic1ΔC does not appear in the same reaction time upon addition of Cks1 with mutations to the phosphate-binding pocket ("+pocket", R33E S82E R102A) or a Y30E mutation. Stronger bands corresponding to hypophosphorylated forms are instead observed. Use of R75A, T80D, and L83D mutants also results in considerable loss of hyperphosphorylated Sic1ΔC, and intermediate forms containing fewer phosphates are the dominant product. All the mutants are capable of forming a complex with Cdk (Appendix Figure A3b). In reactions with a Sic1ΔC containing a single phosphorylation site (all sites mutated to alanine except T5), the mutants behave similarly to wild-type Cks1 (Figure 2.6a). This control reaction demonstrates that Cks1 mutations that disrupt substrate docking have no effect on the catalytic activity of the kinase towards a single phosphoacceptor site, but instead result in defects specifically in the mechanism of multisite phosphorylation.

To demonstrate directly the function of Cks in priming-dependent phosphorylation, we assayed kinase activity on primed substrates (Figure 2.6b and 2.6c). A Cdc6$^{2-29}$ peptide was synthesized with T7 as a phosphothreonine. We then measured the steady-state kinetics of phosphate incorporation at T23 in the presence of the phosphorylated T7. The K_M for the kinase reaction using Cdk1-Clb5 and wild-type Cks1 is less than that measured for a generic single-site substrate or Sic1 with a single T5 phosphoacceptor site available (Appendix Figure A4). Conversely, the absolute k_{cat} value for the wild-type reaction, calculated in these experiments by comparing V_{max} to the published absolute k_{cat} for the H1 peptide[9], is similar to the k_{cat} for reactions with single-site substrates. We tested in similar reactions Cks1 that contains mutations in the consensus sequence binding residues (Figure 2.6b). These reactions all proceed with K_M values greater than reactions with wild-type protein. As observed in the Sic1ΔC multisite phosphorylation assay, mutations to the cationic pocket or Y30 have the largest effect on K-$_M$, while the T80D, L83D, and R75A mutations all show clear but more modest effects. These data demonstrate that Cks1

residues critical for binding phosphorylated substrates are required for the K_{M-} decrease that results from priming in a multisite kinase reaction.

We also assayed the importance of the Cks-binding consensus in the substrate. Cdc6 peptides with mutations in the phosphoacceptor site or surrounding consensus residues were synthesized and used in kinase reactions with wild-type Cks1 (Figure 2.6c). Mutation of the priming phosphothreonine to an alanine (T7A) leads to a K_M increase for the reaction measuring phosphate incorporation at T23. Consistent with our binding measurements, mutation of the proline in the -2 position of the consensus to a tyrosine (P5Y) does not change the K_M from the wild-type reaction, whereas mutation to a lysine (P5K) increases the K_{M-} by 3-fold. Mutation of the +1 proline (P8A) results in a 6-fold increase in $K\text{-}_M$. These results together further establish the importance of the Cks-substrate association for enhancing Cdk multisite kinetics and demonstrate that a binding consensus, and not solely a phosphate, directs the priming-dependent reaction.

To demonstrate the importance of Cks1 association with specific priming site sequences *in vivo*, we examined the viability of Cks1 mutants that are defective in consensus binding in budding yeast (Figure 2.6d). We identified a mutation (L98S) in Cks1 that has temperature sensitivity at 34ºC. At the restrictive temperature, growth is impaired as described previously[11] but is rescued by wild-type Cks1 expressed from a CEN vector and under control of the alcohol dehydrogenase promoter. In contrast, expression of a phosphate-binding pocket mutant or the consensus-binding mutants fails to rescue the temperature sensitivity.

The Cks-binding consensus is present in a subset of Cdk substrates

To find Cdk substrates that associate with Cks, we considered the sequence (F/I/L/P/V/W/Y) XTP, which contains the minimum requirements for binding Cks1 based on our data. We input this sequence into the Yeast Genome Database Pattern Matching tool (http:// www.yeastgenome.org/cgi-bin/PATMATCH/nph-patmatch). 3263 sequences match the consensus; these sequences are found in 2100 different ORFs (Figure 2.7a). 269 of the

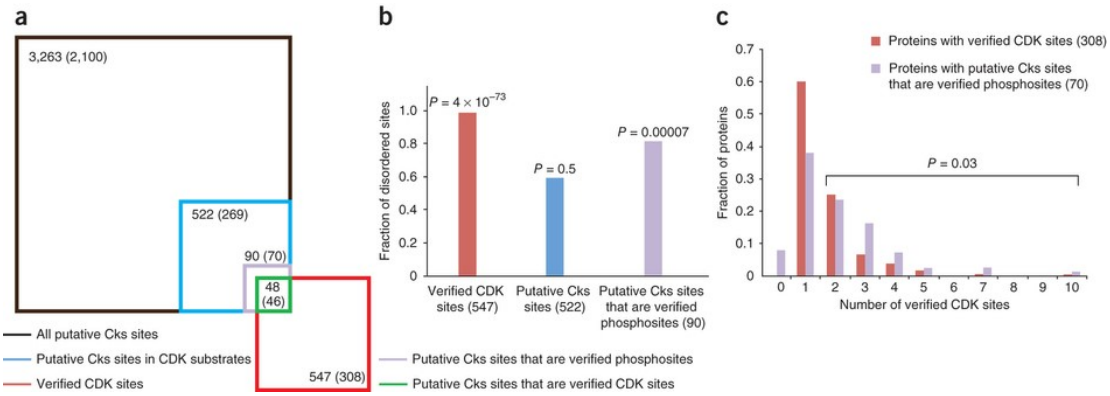

Figure 2.7 Sequence context of putative Cks binding sites. (a) Venn diagram showing in each set the number of sequences that match the minimal Cks consensus (F/I/L/P/V/W/Y-X-T-P) and the number of proteins containing those sequences (in parentheses). The set of all verified Cdk sites is taken from a mass spectrometry based screen5. Square areas are proportional to site number. (b) The fraction of sites found in disordered protein sequences. P values are calculated using the Chi-squared test and assuming an expected distribution equivalent to that found for all (S/T)P sites in the yeast proteome (60.6% disordered)5. (c) Multiplicity of Cdk sites in Cdk and putative Cks-directed substrates. The bars show the number of Cdk sites verified in the mass spectrometry screen5 for all Cdk substrates found in that screen (red) and for substrates that contain putative Cks sequences that are also verified phosphorylation sites (purple). The substrates that contain zero verified Cdk sites in the mass spectrometry screen contain Cks sequences that are phosphorylated according to the PhosphoGRID database. The P value is calculated for a distribution between either zero or one Cdk sites or more than one Cdk site. The Chi-squared test was used assuming an expected distribution for the Cks-containing proteins that is equivalent to the distribution for all verified Cdk sites in the mass spectrometry screen.

2100 ORFS are known Cdk substrates, as determined in at least one of the two global Cdk-substrate identification studies[4,5]. There are 522 putative Cks-binding sequences within these 269 ORFs, which we list in Appendix Table A1.

In order to filter and characterize better the properties of Cks targets, we further analyzed the 522 putative Cks-binding sites found in Cdk substrates (Figure 2.7). We first searched for evidence validating that the sites are phosphorylated by Cdk or other kinases. 48 of the 522 sites were identified as Cdk phosphorylation sites in a mass spectrometry-based proteomics screen to identify Cdk substrates (Figure 2.7a)[5], and 42 other sites were identified as phosphorylation sites in the PhosphoGRID database (www.phosphogrid.org). These 90 Cks consensus sites that correspond to validated phosphorylation sites (highlighted in Supplementary Table 1) are found in 70 different ORFS.

Cdk sites tend to be found in regions of proteins that lack structure[5,41]. We analyzed

whether the Cks consensus sites are in sequences that are likely structured or disordered using a web-based disorder prediction tool[42]. We found that 309 of the 522 putative Cks sites (59%) are in regions of likely disorder, while 73 of the 90 (81%) Cks sites that are verified phosphorylation sites are found in likely disordered regions (Figure 2.7b). When all putative Cks sites are considered, there is no significant preference for disordered sequences; however, the statistics for the subset of Cks sites corresponding to verified phosphorylation sites do suggest that Cks preferentially binds unstructured sequences. The disorder frequency of Cks sites is less than the disorder frequency (99%) of all verified Cdk sites in the mass spectrometry screen[5]. It may be that Cks sites are more likely to be found in predicted structured regions because of the hydrophobic amino acid in the -2 position.

Considering the role of Cks in stimulating multisite phosphorylation kinetics, we predicted and found that Cks sites preferentially occur in substrates that contain multiple Cdk sites. Putative Cks sites that are verified phosphorylation sites occur in substrates with more than one Cdk site at a frequency that is greater than expected from the multiplicity distribution of all Cdk substrates found in the mass spectrometry screen (Figure 2.7c)[5].

Cks mediates Cdk1-directed Wee1 activity at mitotic entry

In examining the list of putative Cks binding partners, we found the potential docking association of Cks1 with budding yeast Wee1 (called Swe1) of particular interest, as Swe1 is known to form a phosphorylation-dependent complex with Cdk1 during mitotic entry. This complex is required for efficient inhibitory phosphorylation of Cdk1 by Swe1 on Y19[22,31,32]. Formation of the complex requires phosphorylation of 8 consensus sites in Wee1 by Cdk1[32]. Similar mechanisms are likely to act in vertebrate cells[31,43,44]. We hypothesized that Cks docking to specific phosphorylated consensus sites mediates the Cdk1-Wee1 complex, and we tested this idea with mutational analysis of Swe1 in budding yeast.

Of the eight consensus Cdk1 phosphosites in Swe1, there are four phosphothreonines: T45,

T121, T196, and T373. All except T45 possess a bulky hydrophobic residue in the -2 position, and T196 and T373 were previously found to play an important role in Cdk1 complex formation in budding yeast[32]. Although neither the precise sequences surrounding the sites nor their location in the primary sequence are conserved in higher eukaryotes, most Swe1 orthologs contain 3 or 4 putative Cks binding sites. We tested Cks1 binding to each of these phosphopeptides by ITC and found as predicted that all except T45 bound with an affinity similar to phosCdc6$^{2-10}$ (Table 1). To assay the importance of the Cks-binding sites *in vivo*, a yeast strain was constructed in which the three consensus threonines in Swe1 were mutated to serines (T121S, T196S, T373S; "triple mutant"), which preserves Cdk phosphorylation of Swe1 but inhibits Cks association. We observed no considerable difference in the phosphorylation pattern of mutant and wild-type Swe1 (Figure 2.8) following release from G1 arrest, suggesting that the Cks consensus sites do not play a role in Swe1 hyperphosphorylation *in vivo.* The triple mutant cells do show a defect in phosphorylation of Cdk1 on Y19 (Figure 2.8). The decreased Cdk1 phosphorylation is not due to reduced Swe1, as the total amount of Swe1 and its phosphorylation state are consistent between mutant and wild-type cells (Figure 2.8). We conclude that the Cks consensus sites are critical for Swe1 activity towards Cdk1. The fact that hyperphosphorylation of Swe1 appears to be normal in the mutant suggests that Cks1 binding does not influence multisite phosphorylation in this context. Rather, Cks1 mediates

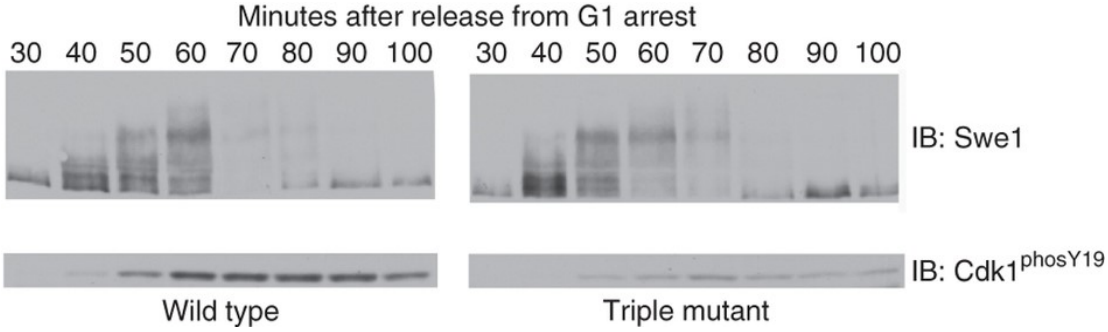

Figure 2.8 Cks consensus sites in Wee1 are required for Cdk1 inhibitory phosphorylation. Yeast expressing wild-type and mutant (T121S, T196S, T373S) Wee1 (Swe1) were released from a G1 arrest. Cells at the indicated time points were lysed and Swe1 (a) and phosphorylation on Cdk1 Y19 (b) were probed. Exposures of the full gels for this experiment can be seen in Supplemental Figure 7c. (Rafael Lucena)

formation of the complex in response to Cks1-consensus site phosphorylation, which in turn allows Swe1 to phosphorylate Cdk1 efficiently on its inhibitory site.

Discussion

Although it has been postulated that Cks stimulates Cdk activity by binding primed substrates[3,12], little evidence has been provided for this model, and the association of Cks with phosphorylated substrates has not been well characterized. We demonstrate here that Cks binds phosphorylated Cdk substrates in a sequence dependent manner and find that efficient hyperphosphorylation of substrates depends on recognition of sequence elements that surround the phosphate. Our results support a model in which Cks binds specific priming sites to facilitate phosphorylation at other sites (Figure 2.9a). Other data suggest that Cks1 orients substrates for Cdk phosphorylation at sites that are C-terminal to the Cks1 binding site (M.K. and M.L. unpublished). Characterization of the Cks-binding consensus sequence has permitted identification of a large set of Cdk substrates (269 proteins containing 522 Cks sites) that may utilize the Cks-dependent hyperphosphorylation mechanism. Considering that a smaller subset of putative Cks-binding sites contains sites for which phosphorylation has been directly observed (90 sites in 70 proteins), we anticipate that the actual number of Cks-interacting substrates in the cell is more modest. It remains an open question how many real Cks-directed Cdk substrates exist, and it will be interesting to explore the different cell cycle contexts in which Cks contributes to the desired signaling response.

The observation that only a subset of Cdk sites have the required surrounding sequence for Cks binding has important implications for our understanding of multisite phosphorylation in cell cycle regulation. The data presented here demonstrate that Cdk phosphoacceptor sites differentially influence the kinetics of phosphate incorporation at other sites. This regulatory mechanism can be used to control whether and when sites with critical outputs are phosphorylated. For example, in Sic1, phosphorylation at specific sites required for ubiquitylation and degradation requires priming phosphorylation at the Cks consensus site

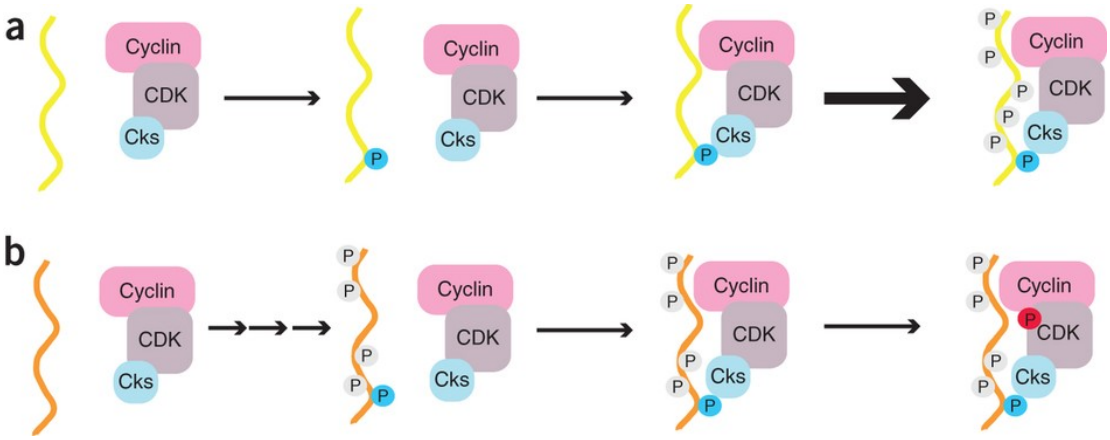

Figure 2.9 Cks is a specificity factor that mediates Cdk-substrate association for multiple functions. a) Cks binds substrates phosphorylated at specific consensus sites (blue phosphate), and the Cks-Cdk-substrate complex stimulates further phosphorylation. The stimulatory effect requires that the Cks-consensus site be phosphorylated early in the reaction, as is true in Sic1. b) Cks acts as an adaptor that targets Cdk to its regulators. In the case of Wee1, association with Cks consensus sites induces inhibitory phosphorylation in Cdk (red phosphate).

(M.K. and M.L. unpublished). It has also been shown recently that different phosphorylation events in the Retinoblastoma protein induce distinct conformational changes[26], which motivates the need for unique control of phosphorylation at distinct sites. This notion that specific phosphorylation sites play distinct roles in tuning signaling outputs differs from other models for the mechanism of multisite phosphorylation in the cell cycle[21,23], in which phosphorylation sites play generic roles.

Our data suggest that the influence of Cks on Cdk substrate phosphorylation kinetics depends on whether Cks-binding consensus sites are phosphorylated early or late in the multisite reaction. In the case that a Cks-binding site is phosphorylated early, phosphorylation triggers Cks binding to enhance phosphorylation of remaining sites (Figure 2.9a). The consensus for optimal Cks1 affinity contains a Cdk acceptor site (TP), which is consistent with a self-priming mechanism. We note that other kinases could phosphorylate the Cks consensus, including MAP kinases, which also recognize TP[45]. The scenario depicted in Figure 7a is true for Sic1. Two optimal Cdk sites that act as Cks-dependent priming (T5 and T33) sites are required for semiprocessive phosphorylation of Sic1 and its degradation[24]. Cdc25 phosphorylation also uses the priming mechanism; mutation of Cks

consensus sites abrogates cooperativity in the phosphorylation kinetics[25]. Alternatively, if Cks consensus sites are phosphorylated late in the multisite reaction, Cdk phosphorylation proceeds without or with limited Cks-induced stimulation for that particular substrate (Figure 2.9b). Swe1/Wee1 may be an example of such a substrate. We observe no effect on Swe1 hyperphosphorylation *in vivo* when the Cks consensus is disrupted, and it has been proposed that the best Cks consensus sites (T196 and T373) are phosphorylated late[33].

We found that the Cks consensus in budding yeast Wee1 is required for its ability to phosphorylate Cdk on the inhibitory Y19 site. This observation demonstrates a novel role for Cks in regulation of Cdk activity through influencing posttranslational modifications and explains one mechanism by which Cks regulates mitotic entry. It also emphasizes that the cellular role of Cks extends beyond its capacity to stimulate Cdk kinetics. Cks mediates phosphorylation-dependent interactions between Cdk and its own regulators (Figure 2.9b). The Wee1-Cdk1 complex is a second example of this function in addition to hsCks1 binding phosphorylated p27 (phosp27) within a ubiquitin ligase[18-19].

The structure of hsCks1 bound to phosp27 in the context of the Skp2-Skp1-Cullin ligase was previously solved[36], and comparison with the phosCdc6-Cks1 structure here indicates several similarities (Appendix Figure A5). The location of the phosphothreonine phosphate and γ-methyl groups and contacts with the +1 proline are equivalent. One notable difference is the presence of a glutamate in the -2 position in phosp27, which is not preferred in the Cks1 binding consensus. In the phosp27-hsCks1-ligase structure, this phos27 E185 hydrogen bonds with R294 and Y346 of Skp2 and Q52 of hsCks1. In Cks1, L83 is in the equivalent position as Q52. This difference explains why glutamate in the -2 position facilitates the phosp27-hsCks1 interaction in the context of ubiquitylation, whereas a hydrophobic residue is required for general Cks1 binding to phosphorylated targets. HsCks2 has a leucine at the hsCks1-Q52 position, which is similar to Cks1, the fission yeast ortholog suc1, and the frog ortholog p9. Our observations suggest that hsCks2, like its more distant orthologs, has a general role in Cdk binding to its substrates and regulators, while Cks1 has

evolved to gain its specific function as an adaptor for the Skp2 SCF ligase. Further dissection of the functional differences between the human Cks paralogs will be important for understanding the role of Cks in tumorigenesis and for its use as a cancer diagnostic.

Methods

Protein expression and purification

Wild-type full-length *S. cerevisiae* Cks1 was either expressed untagged or tagged as indicated from a pET vector in *E. coli*. The untagged wild-type protein and the Cks^{1-112}-$phosCdc6^{3-9}$ fusion used for crystallization were purified by ion-exchange chromatography and size-exclusion chromatography, and the hexahistadine-tagged protein was purified with nickel-NTA chromatography followed by ion-exchange chromatography. The GST-tagged protein was purified with glutathione sepharose resin followed by ion-exchange chromatography. The GST-tag was then cleaved by GST-tagged TEV protease, and the GST-TEV and cleaved GST tag were separated from Cks1 with glutathione sepharose. The *S. cerevisiae* $Cdc6^{1-48}$ peptides were all expressed as hexahistadine fusion constructs and purified as described for His-tagged Cks. Cdk6–CycV or Cdk2–CycA were used as previously described to phosphorylate purified proteins for calorimetry and crystallization[46]. Quantitative phosphate incorporation was verified by electrospray mass spectrometry in all cases, with the exception that for wild-type $Cdc6^{1-48}$, we could at most achieve a maximum of three phosphates added and determined that our sample was a mixture of peptides containing three out of four sites phosphorylated. This mixture is consistent with our observation of a stoichiometry slightly less than n = 2.

For kinase assays, N-terminally His-tagged recombinant Sic1ΔC (aa 1-215) protein was purified by cobalt affinity chromatography. Clb5-Cdk was purifired with TAP tag method was used as described previously[4]. Wild-type Cks1 and Cks1 +pocket mutant (R33E S82E R102A) used in kinetics assays were purified as described[47].

Peptide spot binding assays

Synthetic phosphopeptides were resuspended in PBS pH 7.4 to a concentration of 1.8 mM and covalently coupled to 1 mg/ml BSA by stirring with an equal volume of 0.2%

glutaraldehyde at room temperature. Reactions were quenched after 1 hour with an equal volume of 1M glycine and samples were dialyzed against 25 mM Tris-HCl pH 7.4, 150 mM NaCl. Small volumes (0.5-3 µl) peptide samples were spotted onto methanol-activated PVDF membrane. Positional scanning peptide arrays were synthesized on amino-PEG cellulose membranes by the MIT Biopolymers Laboratory. Blocked membranes were probed with 2 µM hexahistadine-tagged Cks, detected with HRP-His Probe (sc-8036), and developed using SuperSignal West Dura ECL reagents.

Crystallization and structure determination

Following phosphorylation, the fusion protein was prepared for crystallization by elution from a Superdex 75 column in a buffer containing 25 mM Tris, 150 mM NaCl, and 1 mM DTT at a concentration of 40 mg/mL. Proteins were crystallized by sitting drop vapor diffusion at 20° C. Crystals grew for 2 weeks in a solution containing 400 mM potassium sodium tartrate, 0.1M MES pH 5.5 and were harvested and flash-frozen in the same solution with 30% glycerol

Data were collected at λ = 1.0332Å, 100K on Beamline 23-ID-D at the Advanced Photon Source, Argonne National Laboratory. Diffraction spots were integrated with Mosflm[48] and scaled with SCALE-IT[49]. Phases were solved by molecular replacement using PHASER[50]. ScCks1 (PDB code: 1qb3) was used as a search model. The initial model was rebuilt with Coot[51], and the Cdc6 peptide was added to electron density visible in the previously described phosphate-binding pocket. The resulting model was refined with Phenix[52]. Several rounds of position refinement with simulated annealing and individual temperature factor refinement with default restraints were applied.

Final Ramachandran statistics:

Outliers : 0.22%

Allowed: 6.70%

Favored: 94.20%

Isothermal Titration Calorimetry

ITC was performed using the MicroCal VP-ITC calorimeter. Cks1 was dialyzed overnight prior to the assay in a buffer containing 150 mM NaCl, 25 mM Tris-HCl (pH 7.4), 1 mM β-mercaptoethanol, and 0.01% NaN_3. In most cases the synthetic phosphopeptides were dialyzed for up to 5 days in the same buffer. $Cdc6^{1-48}$ was buffer exchanged into ITC buffer over Superdex75 on the day of ITC. For experiments with synthetic peptides, phosphopeptides at concentrations □2–6 mM were titrated into Cks1 at a concentration ~50 -100 μM. For experiments with $Cdc6^{1-48}$, Cks1 at a concentration of ~0.5-1 mM was titrated into $Cdc6^{1-48}$ at a concentration of ~30-80 μM. Data were analyzed with the Origin calorimetry software package assuming a one-site binding model. Experiments were repeated 2–4 times, and the reported error is the standard deviation of each set of measurements.

Kinetic Assays

The general composition of the assay mixture was as follows: 50mM Hepes, 180mM NaCl, 5mM $MgCl_2$, 0,2mg/ml BSA, 2% glycerol, 2mM EGTA, 500nM Cks1 and 500uM ATP (with added [γ-32P] ATP (Perkin Elmer)) (PH 7.4). 20 mM imidazole was also added in experiments with protein substrate. Around 1-5 nM of purified Cdk1-Clb5 kinase complex was used. Reactions were initiated by adding preincubation mixture and [γ-32P] ATP to the substrate protein or peptide. Aliquots were collected at least at two different time points and the reaction was stopped by adding the SDS-PAGE sample buffer (in the case of proteins) or 2.5M guanidine hydrochloride (in the case of Biotin labeled peptides). For quantitative phosphorylation assays, the initial velocity conditions were defined as a substrate turnover ranging up to 20% of the total turnover in assays with biotinylated peptides and as 5% in assays with protein substrate. For the assay with different Cks1 mutants, purified kinase complex was preincubated for 45 min with Cks1 proteins. The composition of the

preincubation mixture was as follows: 50 mM Hepes, 150 mM NaCl, 5 mM MgCl2, 0.4 mg/ml BSA 500 uM ATP and 1 mM Cks1 (pH 7.4). For capturing biotinylated peptides SAM2® Biotin Capture Membrane (Promega) was used according to the instructions given by the manufacturer. 10% SDS-PAGE with added PhosTag reagent was used to seperate different Sic1∆C phosphoforms[53]. Sic1∆C concentrations were kept in the range of 1-3 mM, several fold below estimated K_m value.

Budding yeast temperature-sensitivity rescue experiment

A temperature-sensitive Cks1-mutant yeast strain (TS) was created using error-prone PCR and homologous recombination in the wild-type *S. cerevisiae* strain DK186 (WT). The TS strain (containing a L98S mutation) and wild-type strains were transformed with the CEN vector pRS315 containing either wild-type yeast Cks1 or a Cks1 point mutant and grown in selective media to saturation. The transformants were then spot plated at 1:5 serial dilutions on selective media and grown at room temperature or 34°C. All Cks1 expression from the CEN vector was under control of the yeast alcohol dehydrogenase promoter (pADH).

Wee1 and Cdk1 phosphorylation in budding yeast

A strain in which the endogenous SWE1 gene was replaced by Swe1-T121S T196S T373S was generated by transforming a strain carrying wee1**Δ**::URA3 with the full-length wee1-T121S T196S T373S allele excised from a plasmid. Loss of the URA3 gene was selected for by plating on FOA, and was confirmed by PCR and western blot. A control strain was also created by integrating the wild-type copy of the SWE1 gene from a plasmid at the SWE1 locus. The time course and Western blots were performed as previously described[32]. For Swe1 Western blots, electrophoresis was performed on a 10% polyacrylamide gel until a 66.5-kD marker ran to the bottom of the gel. Western blots were transferred for 90 min at 800 mA at 4°C in a transfer tank in a buffer containing 20 mM Tris base, 150 mM glycine,

and 20% methanol. Blots were first probed overnight at 4°C with P-cdc2 (Tyr15 9111L; Cell Signaling Technology, dilution 1:5000) and affinity-purified rabbit polyclonal antibodies raised against a Swe1 peptide (dilution 1:1000). Blots were then probed with an HRP-conjugated donkey anti–rabbit secondary antibody (GE Healthcare, dilution 1:5000).

Original images of autoradiographs and blots used in this study can be found in Supplementary Figure 7.

Accession code

Coordinates and structure factors for the $Cks1^{1-112}$-$phosCdc6^{3-9}$ fusion protein have been deposited in the Protein Data Bank under accession codes 4LPA.

Acknowledgements

The authors acknowledge R. Cook of the MIT Biopolymers group for synthesis of and E. van Veen for providing valuable advice regarding peptide arrays. The authors thank E. Chen for assistance with CD experimental design and analysis. This research was supported by funding to S.M.R. from the American Cancer Society (RSG-12-131-01-CCG).

Author contributions

D.A.M., E.R.M.B., M.K., R.L., D.R.K., M.L., and S.M.R. designed the study. D.A.M., E.R.M.B., M.K., R.L., M.V.M., and A.H. performed experiments. All authors analyzed data. D.A.M., E.R.M.B., and S.M.R. wrote the manuscript.

References

1. Ubersax, J.A. & Ferrell, J.E., Jr. Mechanisms of specificity in protein phosphorylation. *Nat Rev Mol Cell Biol* 8, 530-41 (2007).

2. Brognard, J. & Hunter, T. Protein kinase signaling networks in cancer. *Curr Opin Genet Dev* 21, 4-11 (2011).

3. Morgan, D.O. *The cell cycle : principles of control*, xxvii, 297 p. (Published by New Science Press in association with Oxford University Press ;Distributed inside North America by Sinauer Associates, Publishers, LondonSunderland, MA, 2007).

4. Ubersax, J.A. et al. Targets of the cyclin-dependent kinase Cdk1. *Nature* 425, 859-64 (2003).

5. Holt, L.J. et al. Global analysis of Cdk1 substrate phosphorylation sites provides insights into evolution. *Science* 325, 1682-6 (2009).

6. Sherr, C.J. Cancer cell cycles. *Science* 274, 1672-7 (1996).

7. Loog, M. & Morgan, D.O. Cyclin specificity in the phosphorylation of cyclin-dependent kinase substrates. *Nature* 434, 104-8 (2005).

8. Schulman, B.A., Lindstrom, D.L. & Harlow, E. Substrate recruitment to cyclin-dependent kinase 2 by a multipurpose docking site on cyclin A. *Proc Natl Acad Sci U S A* 95, 10453-8 (1998).

9. Koivomagi, M. et al. Dynamics of Cdk1 substrate specificity during the cell cycle. *Mol Cell* 42, 610-23 (2011).

10. Hayles, J., Aves, S. & Nurse, P. suc1 is an essential gene involved in both the cell cycle and growth in fission yeast. *Embo J* 5, 3373-9 (1986).

11. Tang, Y. & Reed, S.I. The Cdk-associated protein Cks1 functions both in G1 and G2 in Saccharomyces cerevisiae. *Genes Dev* 7, 822-32 (1993).

12. Pines, J. Cell cycle: reaching for a role for the Cks proteins. *Curr Biol* 6, 1399-402 (1996).

13. Shapira, M. et al. Alterations in the expression of the cell cycle regulatory protein cyclin kinase subunit 1 in colorectal carcinoma. *Cancer* 100, 1615-21 (2004).

14. Martinsson-Ahlzen, H.S. et al. Cyclin-dependent kinase-associated proteins Cks1 and Cks2 are essential during early embryogenesis and for cell cycle progression in somatic cells. *Mol Cell Biol* 28, 5698-709 (2008).

15. Lan, Y. et al. Aberrant expression of Cks1 and Cks2 contributes to prostate tumorigenesis by promoting proliferation and inhibiting programmed cell death. *Int J Cancer* 123, 543-51 (2008).

16. Westbrook, L. et al. High Cks1 expression in transgenic and carcinogen-initiated mammary tumors is not always accompanied by reduction in p27Kip1. *Int J Oncol* 34, 1425-31 (2009).

17. Ganoth, D. et al. The cell-cycle regulatory protein Cks1 is required for SCF(Skp2)-mediated ubiquitinylation of p27. *Nat Cell Biol* 3, 321-4 (2001).

18. Spruck, C. et al. A CDK-independent function of mammalian Cks1: targeting of SCF (Skp2) to the CDK inhibitor p27Kip1. *Mol Cell* 7, 639-50 (2001).

19. Morris, M.C. et al. Cks1-dependent proteasome recruitment and activation of CDC20 transcription in budding yeast. *Nature* 423, 1009-13 (2003).

20. Yu, V.P., Baskerville, C., Grunenfelder, B. & Reed, S.I. A kinase-independent function of Cks1 and Cdk1 in regulation of transcription. *Mol Cell* 17, 145-51 (2005).

21. Nash, P. et al. Multisite phosphorylation of a CDK inhibitor sets a threshold for the onset of DNA replication. *Nature* 414, 514-21 (2001).

22. Harvey, S.L., Charlet, A., Haas, W., Gygi, S.P. & Kellogg, D.R. Cdk1-dependent regulation of the mitotic inhibitor Wee1. *Cell* 122, 407-20 (2005).

23. Kim, S.Y. & Ferrell, J.E., Jr. Substrate competition as a source of ultrasensitivity in the inactivation of Wee1. *Cell* 128, 1133-45 (2007).

24. Koivomagi, M. et al. Cascades of multisite phosphorylation control Sic1 destruction at the onset of S phase. *Nature* 480, 128-31 (2011).

25. Trunnell, N.B., Poon, A.C., Kim, S.Y. & Ferrell, J.E., Jr. Ultrasensitivity in the Regulation of Cdc25C by Cdk1. *Mol Cell* 41, 263-74 (2011).

26. Burke, J.R., Hura, G.L. & Rubin, S.M. Structures of inactive retinoblastoma protein reveal multiple mechanisms for cell cycle control. *Genes Dev* 26, 1156-66 (2012).

27. Goldbeter, A. & Koshland, D.E., Jr. An amplified sensitivity arising from covalent modification in biological systems. *Proc Natl Acad Sci U S A* 78, 6840-4 (1981).

28. Ferrell, J.E., Jr. Tripping the switch fantastic: how a protein kinase cascade can convert graded inputs into switch-like outputs. *Trends Biochem Sci* 21, 460-6 (1996).

29. Salazar, C. & Hofer, T. Multisite protein phosphorylation--from molecular mechanisms to kinetic models. *Febs J* 276, 3177-98 (2009).

30. Thomson, M. & Gunawardena, J. Unlimited multistability in multisite phosphorylation systems. *Nature* 460, 274-7 (2009).

31. Deibler, R.W. & Kirschner, M.W. Quantitative reconstitution of mitotic CDK1 activation in somatic cell extracts. *Mol Cell* 37, 753-67 (2010).

32. Harvey, S.L. et al. A phosphatase threshold sets the level of Cdk1 activity in early mitosis in budding yeast. *Mol Biol Cell* 22, 3595-608 (2011).

33. Arvai, A.S., Bourne, Y., Hickey, M.J. & Tainer, J.A. Crystal structure of the human cell cycle protein CksHs1: single domain fold with similarity to kinase N-lobe domain. *J Mol Biol* 249, 835-42 (1995).

34. Bourne, Y. et al. Crystal structure of the cell cycle-regulatory protein suc1 reveals a beta-hinge conformational switch. *Proc Natl Acad Sci U S A* 92, 10232-6 (1995).

35. Bourne, Y. et al. Crystal structure and mutational analysis of the human CDK2 kinase complex with cell cycle-regulatory protein CksHs1. *Cell* 84, 863-74 (1996).

36. Hao, B. et al. Structural basis of the Cks1-dependent recognition of p27(Kip1) by the SCF(Skp2) ubiquitin ligase. *Mol Cell* 20, 9-19 (2005).

37. Patra, D., Wang, S.X., Kumagai, A. & Dunphy, W.G. The xenopus Suc1/Cks protein promotes the phosphorylation of G(2)/M regulators. *J Biol Chem* 274, 36839-42 (1999).

38. Mimura, S., Seki, T., Tanaka, S. & Diffley, J.F. Phosphorylation-dependent binding of mitotic cyclins to Cdc6 contributes to DNA replication control. *Nature* 431, 1118-23 (2004).

39. Odaert, B. et al. Solution NMR study of the monomeric form of p13suc1 protein sheds light on the hinge region determining the affinity for a phosphorylated substrate. *J Biol Chem* 277, 12375-81 (2002).

40. Crowley, P.B. & Golovin, A. Cation-pi interactions in protein-protein interfaces. *Proteins* 59, 231-9 (2005).

41. Tyanova, S., Cox, J., Olsen, J., Mann, M. & Frishman, D. Phosphorylation variation during the cell cycle scales with structural propensities of proteins. *PLoS Comput Biol* 9, e1002842 (2013).

42. Ishida, T. & Kinoshita, K. PrDOS: prediction of disordered protein regions from amino acid sequence. *Nucleic Acids Res* 35, W460-4 (2007).

43. Mueller, P.R., Coleman, T.R. & Dunphy, W.G. Cell cycle regulation of a Xenopus Wee1-like kinase. *Mol Biol Cell* 6, 119-34 (1995).

44. Tang, Z., Coleman, T.R. & Dunphy, W.G. Two distinct mechanisms for negative regulation of the Wee1 protein kinase. *EMBO J* 12, 3427-36 (1993).

45. Mukhopadhyay, N.K. et al. An array of insulin-activated, proline-directed serine/ threonine protein kinases phosphorylate the p70 S6 kinase. *J Biol Chem* 267, 3325-35 (1992).

46. Burke, J.R., Deshong, A.J., Pelton, J.G. & Rubin, S.M. Phosphorylation-induced conformational changes in the retinoblastoma protein inhibit E2F transactivation domain binding. *J Biol Chem* 285, 16286-93 (2010).

47. Reynard, G.J., Reynolds, W., Verma, R. & Deshaies, R.J. Cks1 is required for G(1) cyclin-cyclin-dependent kinase activity in budding yeast. *Mol Cell Biol* 20, 5858-64 (2000).

Chapter 3: Speedy interacts with the CDK T-loop to produce phosphorylation-independent CDK activity

Several noncanonical CDK regulators have been discovered that play a role in cancer initiation and progression. We have investigated the structure and activity of the CDK regulator protein SpdyA (Speedy). Speedy functions to activate CDK, it's overexpression enhances cell proliferation, and is implicated in hepatocellular carcinoma, lymphoma, malignant glioma, ovarian cancer, and breast cancer.[1-6] Speedy is able to activate CDK regardless of the normally-required T-loop phosphorylation. Speedy also confers expanded specificity to CDK[7], implying that Speedy can target noncanonical CDK substrates. The molecular mechanisms of CDK activation by Speedy are not well understood. The work contained in this dissertation elucidates some of the molecular details of CDK activation by Speedy and portrays Speedy as a potent CDK activator whose expression overrides normal inhibitory cell cycle signaling.

Speedy is a new member of a class of proteins that is able to replace Cylins in the primary level of CDK activation. The first member of this class to be discovered was p35. p35 is a neuron-specific activator of CDK5 and activates it independent of activation-loop phosphorylation. CDK5 is thought to play little role in cell cycle regulation but instead is required in sensory pathways. p35 shares no homology with Cyclins and CDK5/p35 complex participates in circadian clock regulation.[8] The other member of the class of Cyclin usurpers include viral Cyclins, which share about 30% sequence identity with human Cyclins. They activate CDK regardless of correct cell-cycle signals and contribute to oncogenesis. Given their high sequence identity with the human genes, it is likely that they are derived from cellular Cyclins.[9]

The most recently-discovered of the non-Cyclin CDK activators is Speedy. It is the only endogenous non-Cylin CDK activator that has a role in cell cycle progression throughout all tissues. Speedy shares no significant sequence homology with Cyclins. There are at least five different human Speedy homologs which, while expressed in distinct tissues, are all

highly expressed in testis.[10] Speedy A is the only isoform which is ubiquitously expressed in somatic tissues. The normal role of Speedy is not well understood. In most tissues Speedy is expressed at low level early in the cell cycle at the G1-S transition.[1] Speedy seems to act in concert with other known cell cycle regulators to signal entry into the cell cycle, and is then degraded at the G2/M transition. Expression of non-degradable forms of Speedy induces unregulated cell proliferation.[11] Speedy overexpression is found in cancer and is implicated in tumorigenesis. In laboratory cell lines, overexpression of Speedy induces faster cell cycle progression than control cells. Speedy does this by binding to CDK and activating it in a Cyclin-independent manner.

All Speedy isoforms contain a highly-conserved domain of about 130 amino acids called the Speedybox. The Speedybox is required for Cdk binding[10], but reports of the domains required for Cdk activation by Speedy A differ depending on the species tested. One report shows that the Xenopus Speedybox alone can activate CDK to the same extent as full length Speedy.[12] It was reported elsewhere that mouse Speedybox alone cannot activate CDK, and that the C-terminus is also required.[10] Given that the sequences of mouse and human Speedy proteins are nearly identical, it could be expected that human Speedybox cannot activate CDK. Unexpectedly, the results within this dissertation show that human Speedybox can activate Cdk2 and a high-resolution structure reveals that mechanism of Cdk activation by human Speedybox.

An important functional difference between Speedy and Cyclin is that full activation of the CDK/Cyclin complex requires additional signaling input resulting in CDK T-loop phosphorylation.[13-20] In contrast, the CDK/Speedy complex is active without CDK phosphorylation.[7, 21] (Figure 3.1) Also, CDK is normally inhibited by $p27^{Kip}$ binding, yet the CDK/Speedy complex retains activity when bound to p27[22]. Therefore, Speedy is a potent CDK activator whose expression overrides normal inhibitory cell cycle signaling. In order to understand Speedy's role in cancer it is important to understand the molecular details of how Speedy activates CDK to increase cell cycle progression. The following biophysical

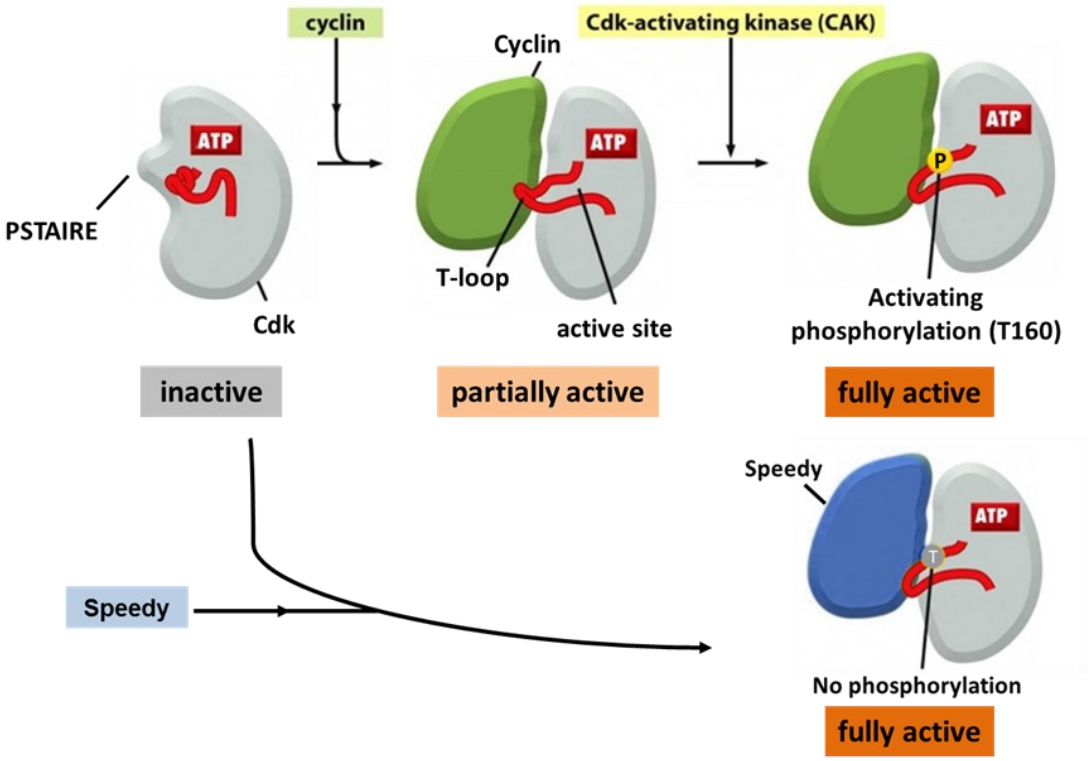

Figure 3.1 Speedy activates CDK in the absence of T160 phosphorylation. Cyclin interacts with the Cdk PSTAIRE helix in to create a partially active kinase complex. Full Cyclin activation of Cdk depends of phosphorylation of T160 on the Cdk T-loop whereas Speedy activation of Cdk does not. (Adapted from Figure 17-17 Molecular Biology of the Cell (© Garland Science 2008)

studies of Speedy provide the first high-resolution structural information that informs how Speedy activates CDK.

Results

Human Speedybox activates Cdk2

Various Speedy constructs have been shown to activate Cdk under various conditions.[7, 10, 12, 21] To test whether we could recapitulate this reported activity *in vitro*, we created a human Speedy A construct (G61-D213) that aligns with the Xenopus Speedybox sequence that is reported to confer full activity to Cdk2. We used bacterially-expressed Speedybox and human CDK2 in assays of kinase activity. (Figure 3.2) We found that bacterially-expressed

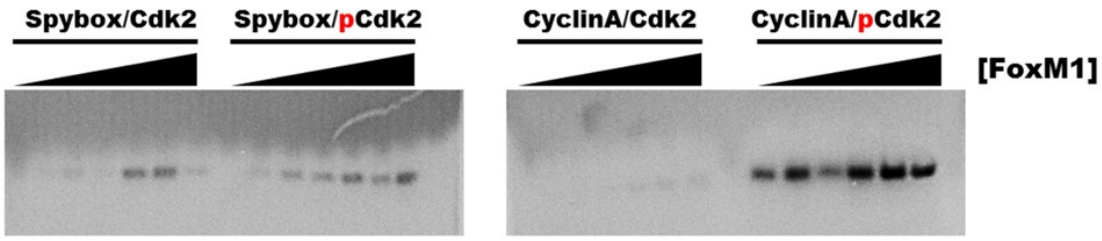

Figure 3.2 Speedy activates Cdk2 regardless of Cdk2 phosphorylation state. Radioactive kinase assays were carried out with 75nM of each kinase complex noted (where the red "p" indicates Cdk2 phosphorylated on T160) and increasing concentrations of a model substrate FoxM1 526-748. From left to right for each kinase, the concentrations of FoxM1 are as follows: 0.5uM, 1uM, 2uM, 4uM, 6uM, 8uM.

CDK2 can be activated by Speedy and that the rates of kinase activity are independent of the phosphorylation states of the T-loop. In contrast, our CDK2 construct is robustly activated by Cyclin A only when the T-loop is phosphorylated. (Figure 3.1) Of note, it has been reported that mouse Speedybox alone is not able to activate CDK2[10] while xenopus Speedybox alone is able to activate CDK2.[12] Our kinetic assays show CDK2 activation by human Speedybox alone.

Speedy's Cdk-interacting helices adopt a cyclin-like structure

We then determined the 2.7Å crystal structure of the Speedybox bound to CDK2. (Appendix Table A2) Human Speedybox is composed of a cluster of helices that bind to the same Cdk2 interface which binds to Cyclin, supporting previous findings that Speedy substitutes for Cyclin in Cdk activation. Cdk2 bound to Speedy is in an active conformation as shown by overlaying the structure with Cdk2 bound to Cyclin A and a substrate peptide. (Figure 3.3) Despite the poor sequence conservation between Speedy and Cyclin A, the three helices (here called A, B, and C) that form the bulk of the CDK interactions are structurally similar. (Figure 3.4b) Helix A doesn't contact CDK2, but makes hydrophobic interactions with Helices B and C. The C-terminus of Helix B makes hydrophobic contacts with the CDK2 PSTAIRE helix and Helix C has multiple polar and van der Waals contacts with the PSTAIRE helix. Speedy interacts with Cdk PSTAIRE in a novel way.

The details of Speedy's interaction with the PSATIRE helix differs from Cyclin although the

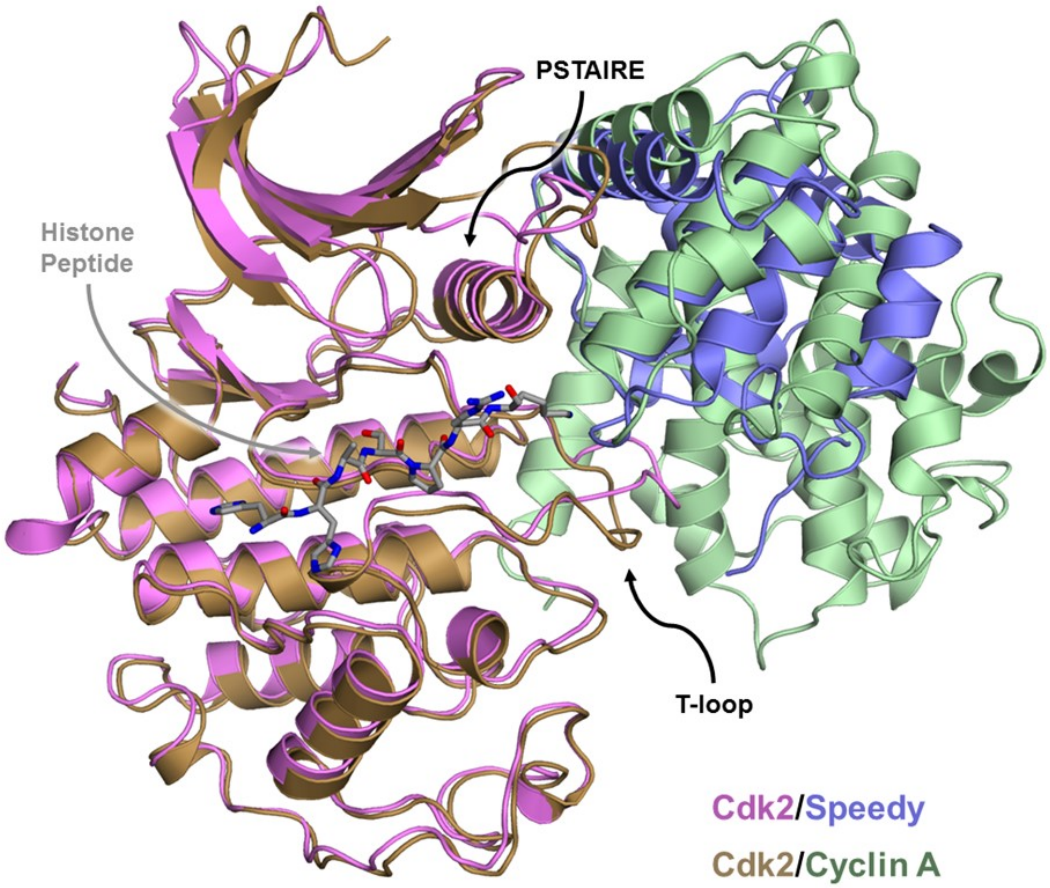

Figure 3.3 Cdk2/Speedy overlayed with Cdk2/Cyclin A/Histone peptide. The Speedy/Cdk2 complex overlays with the fully active Cyclin A/Cdk2/Histone H1 peptide complex (1QMZ), showing that Speedy binds to Cdk2 in a manner similar to Cyclin. The Cdk2 PSTAIRE helix if in the active conformation. Although the T-loop residues are not blocking the active site, there are clear differences in the conformation of the T-loop where it interacts with Cyclin A vs Speedy.

backbone of helices A, B, and C are structurally conserved. (Figure 3.4b) Cyclin A residues found to be important for PSTAIRE binding[23] are not conserved in Speedy. Speedy R164 H-bonds Cdk2 V44 peptide carbonyl while Cyclin E295 H-bonds with the peptide amine of V44. Speedy D165 H-bonds with the peptide amine Cdk2 V44 while Cyclin A H296 π-stacks with Cdk2 H71. One example of identical residues for PSTAIRE binding is Speedy L129 which overlays with Cyclin A L263. Both form van der Waals contacts with Cdk2 I49. Any other sequence identity conservation between Speedy and Cyclin A in these helices does not function to contact the PSTAIRE helix, but are likely to be necessary for the correct

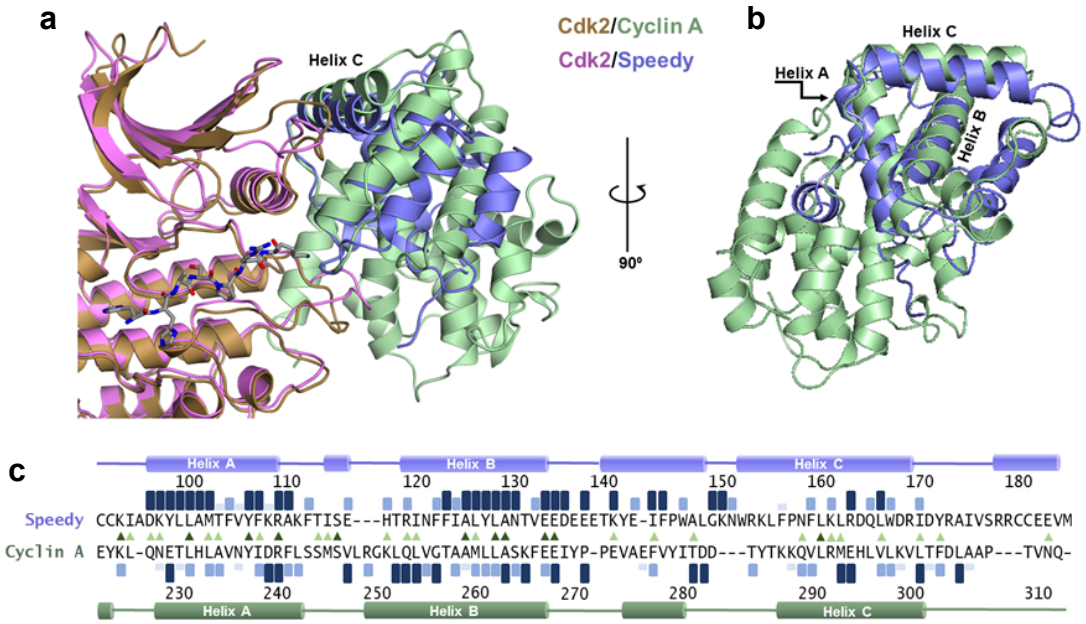

Figure 3.4 The Cdk-interacting interface of Speedy adopts a cyclin-like fold despite lack of sequence conservation between Cyclin A and Speedy A.
Three speedy helices (A, B and C) overlay well with Cyclin A bound to Cdk2. The structural overlay of the helices are aligned by sequence, showing which residues in Helix A, B, and C are structurally aligned. Dark green triangles indicate identical residues. The light green triangles indicate chemically-similar residues. The blue histograms above and below indicate conservation within the respective families of proteins across different human homologs.

structural arrangement of the helices. A hydrophobic patch in Cdk2 noted in the first structure of the Cdk2/CyclinA complex[23] is formed by PSTAIRE residues V44, I49, and I52. Cyclin A contacts these residues with its own hydrophobic patch formed by L299 and F304. (Figure 3.5a) In contrast, Speedy inserts W168 into the Cdk hydrophobic patch effectively using it as a hydrophobic cleft. The indole nitrogen of W168 also forms a hydrogen bond with S53 of Cdk2. (Figure 3.5b) This binding structure allows Speedy to interact with the Cdk PSTAIRE helix so that catalytically-required positioning of E51 is the same as is conferred by Cyclin binding.

While the sequence identity between Speedy and Cyclin A is not well-conserved, the chemical nature of many residues is similar. (Figure 3.3c) This similarity allows Speedy to adopt a Cyclin-like fold at the Cdk interface and results in the familiar Cdk structural rearrangement required for kinase activity.

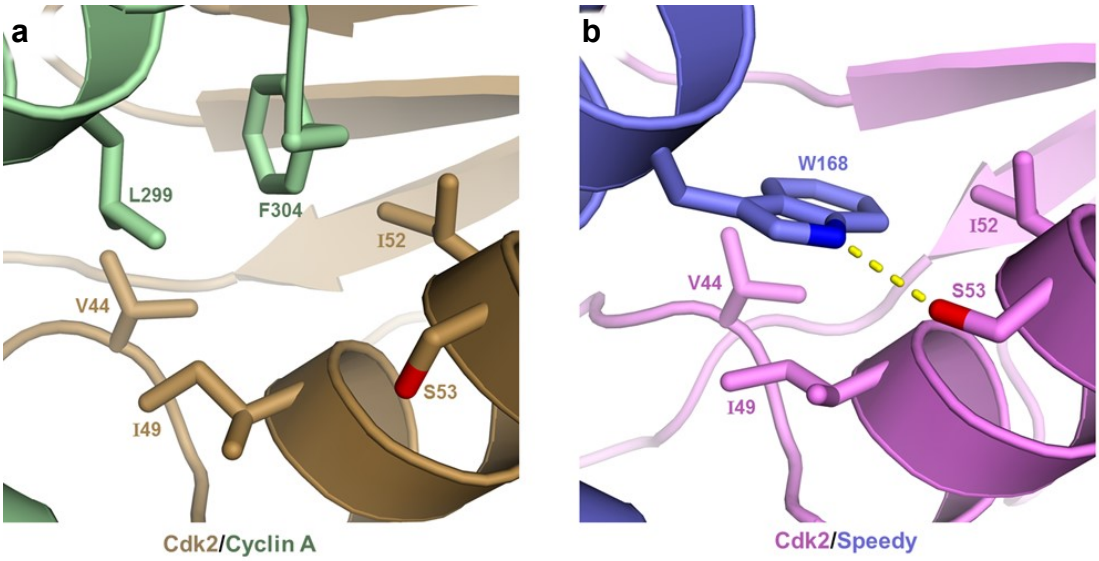

Figure 3.5 Speedy interacts with the Cdk2 PSTAIRE helix in a novel way

Speedy makes multiple unique T-loop interactions

Speedy interacts uniquely with the CDK T-loop to open up the enzyme's active site. The unphosphorylated T-loop adopts an active conformation when compared to the unphosphorylated T-loop of CDK2 bound to Cyclin A. (Figure 3.6) In fact, the T-loop residues T153-158 adopt a conformation not seen in the crystal structures that are thought to represent the different activation states of CDK2. (1FIN, 1QMZ, etc.). The backbone of these residues overlay well with the backbone of the activation loop of CDK5 bound to p35 , indicating that the mechanism of phosphorylation-independent CDK activation is conserved despite the lack of sequence conservation between Speedy and p35.

There appear to be several unique polar-contact networks that contribute to the Speedy-bound T-loop conformation. One hallmark of the fully active Cdk2/CyclinA complex is the triad of Cdk2 arginines 50, 126, and 150 that coordinate the phosphorylated T160 of Cdk2. (Figure. 3.7a) Unphosphorylated, T160 is rotated away from these arginines, which adopt different and disperse H-bonds. When Cdk2 is bound to Speedy, this triad coordinates Speedy residue D136, which then hydrogen bonds with the Cdk T160 peptide amine. (Figure 3.7b) This causes unphosphorylated T160 to adopt a conformation that is

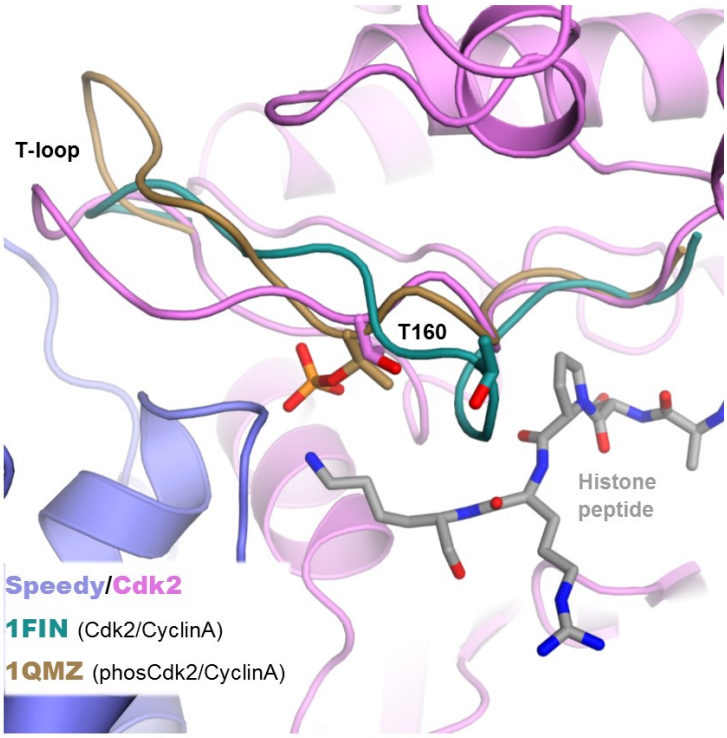

Figure 3.6 The Cdk/Speedy T-loop adopts a novel active conformation
The unphosphorylated T160 of Speedy/Cdk2 overlays with the phosphorylated T160 of CyclinA/Cdk2 T-loop (1QMZ), which is the active conformation of Cdk2. This conformation allows substrates to bind, as shown by the Histone H1 peptide in 1QMZ. In contrast, the inactive conformation of the unphosphorylated T160 of the CyclinA/Cdk2 T-loop (1FIN) blocks substrate binding to the active site. The Speedy/Cdk2 T-loop residues distal to the active site adopt a conformation not seen in structures of Cdk2/ CyclinA.

identical to the phosphorylated T160 seen in the Cdk2/Cyclin A structures. T-loop R150 and PSTAIRE R50 make multiple H-bonds with Speedy sidechains E134 and D136 as well as the peptide carbonyls of E134, E135, and T132. (Figure 3.7c and d) Although some of the residues that contact Cdk2 R150 and R50 are conserved between Speedy and Cyclin A, the position and hydrogen-bonds of R150 and R50 change in Cdk2/CyclinA dependent on whether the activating T160 phosphorylation is present .

Speedy D97 forms a salt bridge with T-loop R157, an interaction which has no analogy in Cdk2/CyclinA structures. Also, Speedy E135 makes polar contacts with T-loop T158 sidechain oxygen and peptide amine, another interaction that is not preserved in Cdk2/ CyclinA. These interactions appear to be critical to the novel active T-loop conformation. To show that Speedy D97 and E135 are critical for Cdk2 activity, I made a Speedy mutant (D97N, E135Q) that is predicted to not activate Cdk2. I used this Speedy mutant/Cdk2 complex in an assay of kinase activity and show that it is inactive compared to Cdk2/ SpeedyBox. (Figure 3.8)

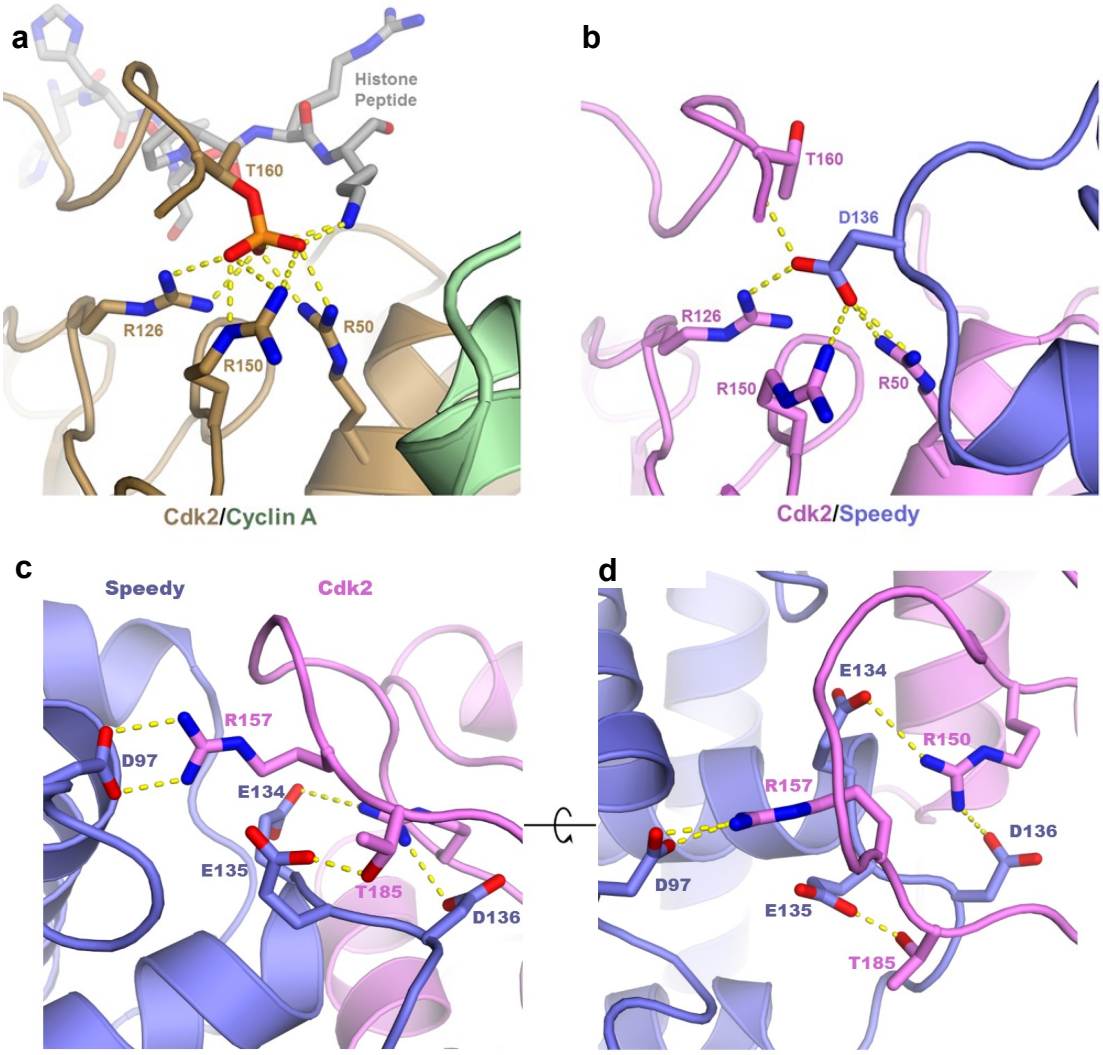

Figure 3.7 Speedy makes multiple unique T-loop interactions

It is known that CDK2/Speedy can bind to but is not inhibited by the CDK inhibitor $p27^{Kip1}$.[22] The mechanism of CDK2/Cycln A inhibition partly relies on $p27^{Kip1}$ binding to the conserved MRAIL motif.[24] When overlayed with the structure of the Cyclin A bound to $p27^{Kip1}$ it is apparent that Speedy cannot form interactions that are structurally analogous to the Cyclin-p27 interactions. To test whether Speedy has specificity toward the p27 residues that bind Cyclins, we should mutate p27 and test for binding to Speedy. Additionally, the work required to obtain a high-resolution crystal structure of the Speedy/CDK2/p27 ternary complex is already underway with promising initial results. The conditions for crystallizing

Figure 3.8 Speedy mutants cannot activate Cdk2. Radioactive kinase assays were carried out with 75nM of each kinase complex noted (where the red "p" indicates Cdk2 phosphorylated on T160) and increasing concentrations of a model substrate FoxM1 526-748. From left to right for each kinase, the concentrations of FoxM1 are as follows: 0.5uM, 1uM, 2uM, 4uM, 6uM, 8uM.

this complex are ripe for improvement through p27 construct boundary trimming and formulation of optimization screens from the initial crystal hits already obtained.

Discussion

The high-resolution structure of the conserved Speedybox reveals that the overall structure of Speedy's CDK2 interaction surface closely resembles that of Cyclins. (Figure 3.4b) The remainder of the Speedybox does not overlay at all with Cyclins, whose structure is well-preserved throughout the family. While the primary sequence is not strictly conserved, the chemical nature of the residues responsible for CDK interaction are conserved. (Figure 3.4c) These facts indicate that Speedy and Cyclins did not evolve from a common gene, but their evolution converged on a structure that functions to activate CDK.

It has been reported that mouse Speedybox alone is not able to activate CDK2 while Xenopus Speedybox alone is able to activate CDK2[10, 12]. In line with the Xenopus findings, our kinetic assays show CDK2 activation by human Speedybox alone. The researchers who did activity assays with mouse Speedy performed alanine scanning to find residues important for binding to CDK2.[10] They found four residues that align with human residues D90, M103, Y107, and F108 whose single amino acid mutations abolish CDK2 binding. It is clear from the crystallography model that these residues stabilize the Speedy structure and do not interact with CDK2. The researchers noted with surprise that alanine mutation of an absolutely conserved EED motif did not result in reduced CDK2 binding. This motif correlates to human E134, E135, and D136 which, combined, make more contacts with the

T-loop than any other set of Speedy residues. It can be reasonably argued that this motif is absolutely required for Speedy activation of CDK.

Previous kinetic assays and ours show reduced CDK2/Speedy activity as compared to pT160-CDK2/Cyclin A. However, the previous assays all utilize verified and ideal CDK substrates. It is known that Speedy changes the specificity of CDK2.[7] Also, the conserved Cyclin MRAIL motif, which confers specificity to CDK through docking interaction[25], is not present in Speedy. With these differences in mind, we can reasonably speculate that we have not found the ideal CDK/Speedy substrate to kinetically compare to known ideal CDK2/ Cyclin A substrates.

Speedy is a fascinating molecule with many biochemical, biophysical, and cellular secrets to unlock. Its role in the cell cycle and its substrates are still a mystery. Valuable collaborators whose specialties include *in vivo* Speedy studies are making great strides toward elucidating Speedy function. These studies point the way toward mechanistic questions suitable for answering using biochemistry and biophysics. I've enjoyed seeing my efforts to answer some of these questions come to fruition and look forward to seeing the results of the work that extends what I have done here.

Methods

Protein expression and purification.

Wild-type *H. sapiens* Speedybox (residues G61-D213) that aligns with the functional XRINGO Speedybox was expressed from a codon-optimized sequence inserted into the pMBP parallel vector in SoluBL21 *E. coli*. Wild-type full-length *H.*sapiens CDK2 was expressed from a pGEX vector. The cells were grown to an OD between 0.6 and 1, cooled in an ice bath for 20min, and expression was induced with 1mM IPTG overnight at 18°C. Cell pellets were resuspended in a wash buffer containing 25mM HEPES pH 7.5, 200mM sodium chloride, 1mM DTT. The resuspended cell lysed together with 1mM PMSF to form the CDK2/SpyBox complex . The clarified lysate was purified with glutathione Sepharose resin. The eluate from the glutathione Sepharose resin was then bound to amylose resin and washed with copious volumes of wash buffer . The tags were then cleaved on-resin overnight by an estimated 10% by mass of GST-tagged TEV protease , and the GST-TEV and cleaved GST tag were separated from CDK2/SpeedyBox complex with glutathione Sepharose. Trace amounts of cleaved MBP was separated from CDK2/SpeedyBox complex with amylose resin. To identify minimal, proteolytically stable components of the complex, it was then subjected to limited proteolysis with 0.01% trypsin for 30min on ice. Trypsinized Speedy was analyzed by electrospray mass spectrometry the results were inconclusive. But a small, stable decrease of mass by SDS-PAGE was hypothesized to represent cleavage at R199, which is close to the end of the functional human Speedybox (S200). Purification of the human Speedybox construct ending at R199 failed on multiple attempts.

Crystallization and structure determination

After trypsinizing, CDK2/SpeedyBox complex was prepared for crystallization by elution from a HiLoad Superdex 200 (GE Healthcare) column in a buffer containing 12.5 mM HEPES pH 7.5, 150 mM NaCl, and 1 mM TCEP at a concentration of 5 mg/mL.

Proteins were crystallized by sitting-drop vapor diffusion at 20 °C. Two different crystal forms were grown for 4 weeks. The initial dataset was collect from crystal grown in 1M lithium chloride, 12% PEG 6000, and 0.1M MES pH 6.2, harvested and flash frozen in the same solution with 20% PEG 200. Data were collected at λ = 1.0332Å, 100 K on Beamline 23-ID-D at the Advanced Photon Source, Argonne National Laboratory. Diffraction spots were integrated with Mosflm[49] and scaled with SCALE-IT[28]. Phases were solved by molecular replacement with PHASER[51]. CDK2 (PDB1QMZ) was used as a search model. The initial model was rebuilt with Coot[30], and Speedy was added to the unmodeled electron density. The resulting model was refined with Phenix[31]. Several rounds of position refinement with simulated annealing and individual temperature-factor refinement with default restraints were applied .

The second crystal form was collected from a solution containing 900mM potassium sodium tartrate, 200mM lithium sulfate, and 0.1 M CHES pH 9.3. The crystals were harvested and flash frozen in the same solution with 15% glycerol. The data were collected and processed as above, using the initial structure as a search model in molecular replacement.

Kinase Assays

Kinase assays were carried out at room temperature in kinase buffer 25mM HEPES pH 7.5, 150mM NaCl, 10mM $MgCl_2$, 1mM DTT. Kinases used were either GST-tagged Cdk2 complexed with either MBP-tagged Speedy or MBP-tagged CyclinA and had a final concentration of 150nM. Kinases were placed in the bottoms of reaction tubes. Master mixes were made with protein substrate, 100μM ATP, kinase buffer, and 0.5μL [γ-32P]-ATP (Perkin Elmer) per 30uL of final reaction volume. Reaction were initated by adding Master mix to reaction tub that contained kinase. Reactions were quenched by adding an equal volume of SDS-PAGE sample buffer.

References

1. Porter, L. A.; Dellinger, R. W.; Tynan, J. A.; Barnes, E. A.; Kong, M.; Lenormand, J. L.; Donoghue, D. J., Human Speedy: a novel cell cycle regulator that enhances proliferation through activation of Cdk2. *J Cell Biol* **2002,** *157* (3), 357-66.

2. Lu, S.; Liu, R.; Su, M.; Wei, Y.; Yang, S.; He, S.; Wang, X.; Qiang, F.; Chen, C.; Zhao, S.; Zhang, W.; Xu, P.; Mao, G., Spy1 participates in the proliferation and apoptosis of epithelial ovarian cancer. *J Mol Histol* **2016,** *47* (1), 47-57.

3. Ke, Q.; Ji, J.; Cheng, C.; Zhang, Y.; Lu, M.; Wang, Y.; Zhang, L.; Li, P.; Cui, X.; Chen, L.; He, S.; Shen, A., Expression and prognostic role of Spy1 as a novel cell cycle protein in hepatocellular carcinoma. *Exp Mol Pathol* **2009,** *87* (3), 167-72.

4. Hang, Q.; Fei, M.; Hou, S.; Ni, Q.; Lu, C.; Zhang, G.; Gong, P.; Guan, C.; Huang, X.; He, S., Expression of Spy1 protein in human non-Hodgkin's lymphomas is correlated with phosphorylation of p27 Kip1 on Thr187 and cell proliferation. *Med Oncol* **2012,** *29* (5), 3504-14.

5. Zhang, L.; Shen, A.; Ke, Q.; Zhao, W.; Yan, M.; Cheng, C., Spy1 is frequently overexpressed in malignant gliomas and critically regulates the proliferation of glioma cells. *J Mol Neurosci* **2012,** *47* (3), 485-94.

6. Golipour, A.; Myers, D.; Seagroves, T.; Murphy, D.; Evan, G. I.; Donoghue, D. J.; Moorehead, R. A.; Porter, L. A., The Spy1/RINGO family represents a novel mechanism regulating mammary growth and tumorigenesis. *Cancer Res* **2008,** *68* (10), 3591-600.

7. Cheng, A.; Gerry, S.; Kaldis, P.; Solomon, M. J., Biochemical characterization of Cdk2-Speedy/Ringo A2. *BMC Biochem* **2005,** *6*, 19.

8. Kwak, Y.; Jeong, J.; Lee, S.; Park, Y. U.; Lee, S. A.; Han, D. H.; Kim, J. H.; Ohshima, T.; Mikoshiba, K.; Suh, Y. H.; Cho, S.; Park, S. K., Cyclin-dependent kinase 5 (Cdk5) regulates the function of CLOCK protein by direct phosphorylation. *J Biol Chem* **2013,** *288* (52), 36878-89.

9. Mittnacht, S.; Boshoff, C., Viral cyclins. *Rev Med Virol* **2000,** *10* (3), 175-84.

10. Cheng, A.; Xiong, W.; Ferrell, J. E.; Solomon, M. J., Identification and comparative analysis of multiple mammalian Speedy/Ringo proteins. *Cell Cycle* **2005,** *4* (1), 155-65.

11. Al Sorkhy, M.; Craig, R.; Market, B.; Ard, R.; Porter, L. A., The cyclin-dependent kinase activator, Spy1A, is targeted for degradation by the ubiquitin ligase NEDD4. *J Biol Chem* **2009,** *284* (5), 2617-27.

12. Dinarina, A.; Perez, L. H.; Davila, A.; Schwab, M.; Hunt, T.; Nebreda, A. R., Characterization of a new family of cyclin-dependent kinase activators. *Biochem J* **2005,** *386* (Pt 2), 349-55.

13. Solomon, M. J.; Lee, T.; Kirschner, M. W., Role of phosphorylation in p34cdc2 activation: identification of an activating kinase. *Mol Biol Cell* **1992,** *3* (1), 13-27.

14. Fesquet, D.; Labbé, J. C.; Derancourt, J.; Capony, J. P.; Galas, S.; Girard, F.; Lorca, T.; Shuttleworth, J.; Dorée, M.; Cavadore, J. C., The MO15 gene encodes the catalytic subunit of a protein kinase that activates cdc2 and other cyclin-dependent kinases (CDKs) through phosphorylation of Thr161 and its homologues. *EMBO J* **1993,** *12* (8), 3111 -21.

15. Poon, R. Y.; Yamashita, K.; Adamczewski, J. P.; Hunt, T.; Shuttleworth, J., The cdc2-related protein p40MO15 is the catalytic subunit of a protein kinase that can activate p33cdk2 and p34cdc2. *EMBO J* **1993,** *12* (8), 3123-32.

16. Solomon, M. J.; Harper, J. W.; Shuttleworth, J., CAK, the p34cdc2 activating kinase, contains a protein identical or closely related to p40MO15. *EMBO J* **1993,** *12* (8), 3133-42.

17. Solomon, M. J., Activation of the various cyclin/cdc2 protein kinases. *Curr Opin Cell Biol* **1993,** *5* (2), 180-6.

18. Kaldis, P.; Sutton, A.; Solomon, M. J., The Cdk-activating kinase (CAK) from budding yeast. *Cell* **1996,** *86* (4), 553-64.

19. Espinoza, F. H.; Farrell, A.; Erdjument-Bromage, H.; Tempst, P.; Morgan, D. O., A cyclin-dependent kinase-activating kinase (CAK) in budding yeast unrelated to vertebrate CAK. *Science* **1996,** *273* (5282), 1714-7.

20. Thuret, J. Y.; Valay, J. G.; Faye, G.; Mann, C., Civ1 (CAK in vivo), a novel Cdk-activating kinase. *Cell* **1996,** *86* (4), 565-76.

21. Karaiskou, A.; Perez, L. H.; Ferby, I.; Ozon, R.; Jessus, C.; Nebreda, A. R., Differential regulation of Cdc2 and Cdk2 by RINGO and cyclins. *J Biol Chem* **2001,** *276* (38), 36028-34.

22. Porter, L. A.; Kong-Beltran, M.; Donoghue, D. J., Spy1 interacts with p27Kip1 to allow G1/S progression. *Mol Biol Cell* **2003,** *14* (9), 3664-74.

23. Jeffrey, P. D.; Russo, A. A.; Polyak, K.; Gibbs, E.; Hurwitz, J.; Massagué, J.; Pavletich, N. P., Mechanism of CDK activation revealed by the structure of a cyclinA-CDK2 complex. *Nature* **1995,** *376* (6538), 313-20.

24. Hao, B.; Zheng, N.; Schulman, B. A.; Wu, G.; Miller, J. J.; Pagano, M.; Pavletich, N. P., Structural basis of the Cks1-dependent recognition of p27(Kip1) by the SCF(Skp2) ubiquitin ligase. *Mol Cell* **2005,** *20* (1), 9-19.

25. Schulman, B. A.; Lindstrom, D. L.; Harlow, E., Substrate recruitment to cyclin-dependent kinase 2 by a multipurpose docking site on cyclin A. *Proc Natl Acad Sci U S A* **1998,** *95* (18), 10453-8.

26. Leslie, A.G. The integration of macromolecular diffraction data. Acta Crystallogr D Biol Crystallogr 62, 48-57 (2006).

27. Howell, P.L. & Smith, G.D. Identification of Heavy-Atom Derivatives by Normal Probability Methods. Journal of Applied Crystallography 25, 81-86 (1992).

28. Mccoy, A.J. et al. Phaser crystallographic software. Journal of Applied Crystallography 40, 658-674 (2007).

29. Emsley, P. & Cowtan, K. Coot: model-building tools for molecular graphics. Acta Crystallogr D Biol Crystallogr 60, 2126-32 (2004).

30. dams, P.D. et al. PHENIX: a comprehensive Python-based system for macromolecular structure solution. Acta Crystallogr D Biol Crystallogr 66, 213-21 (2010).

31. Kinoshita, E., Kinoshita-Kikuta, E., Takiyama, K. & Koike, T. Phosphate-binding tag, a new tool to visualize phosphorylated proteins. Mol Cell Proteomics 5, 749-57 (2006).

32. Balog, E.R. et al. The structure of a monomeric mutant Cks protein reveals multiple functions for a conserved hinge-region proline. J Mol Biol 411, 520-8 (2011).

33. Richardson, H.E., Stueland, C.S., Thomas, J., Russell, P. & Reed, S.I. Human cDNAs encoding homologs of the small p34Cdc28/Cdc2-associated protein of Saccharomyces cerevisiae and Schizosaccharomyces pombe. Genes Dev 4, 1332-44 (1990).

Appendix

Figure A1. Cks ITC traces

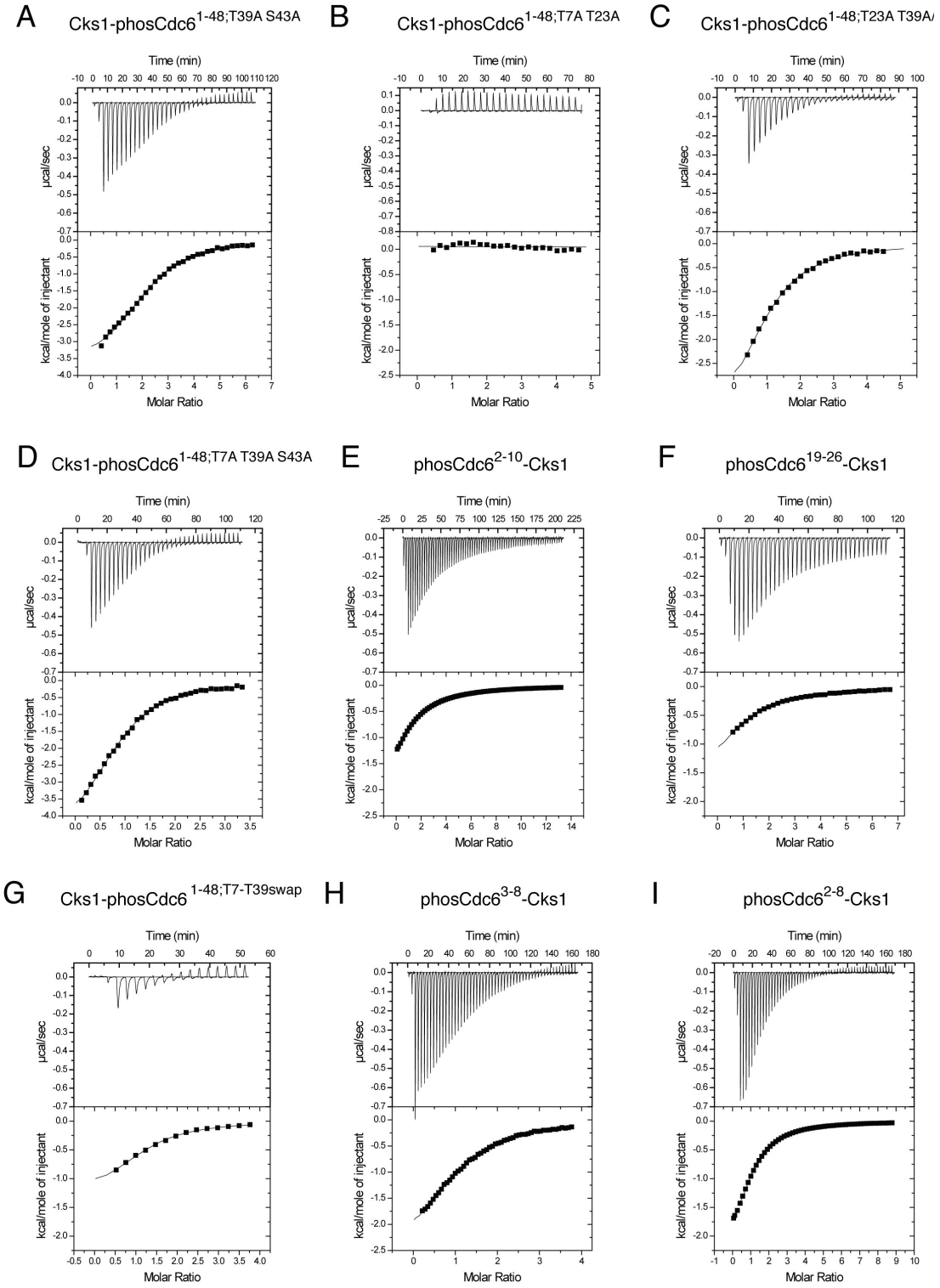

J phosCdc6$^{3-9}$-Cks1

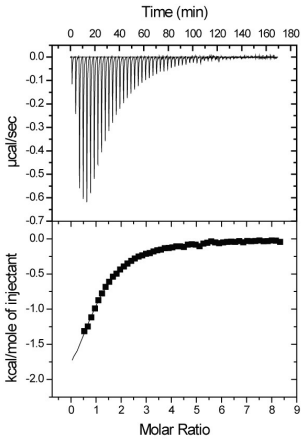

K phosCdc6$^{2-10;\ pT7pS}$-Cks1

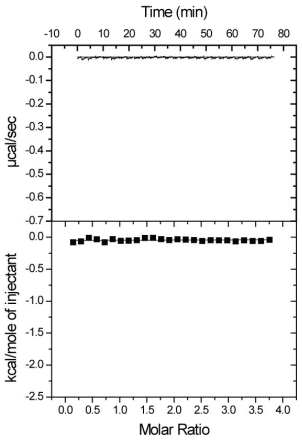

L phosCdc6$^{2-10;\ pT7pY}$-Cks1

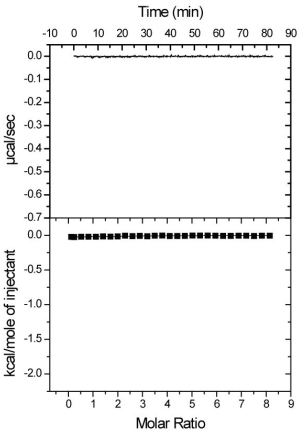

M phosCdc6$^{2-10;\ P8K}$-Cks1

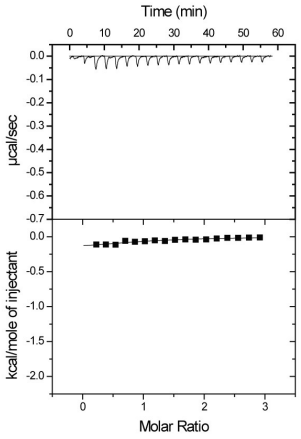

N phosCdc6$^{2-10;\ P5Y}$-Cks1

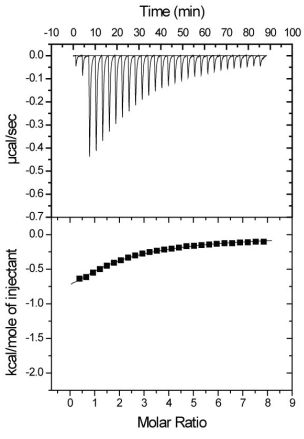

O phosCdc6$^{2-10;\ P5F}$-Cks1

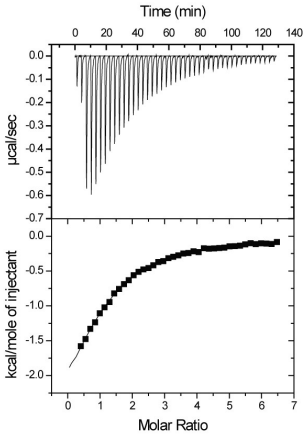

P phosCdc6$^{2-10;\ P5K}$-Cks1

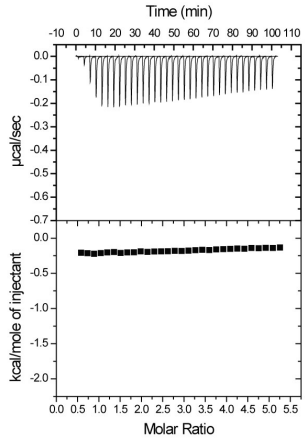

Q phosCdc6$^{2-10;\ T9P}$-Cks1

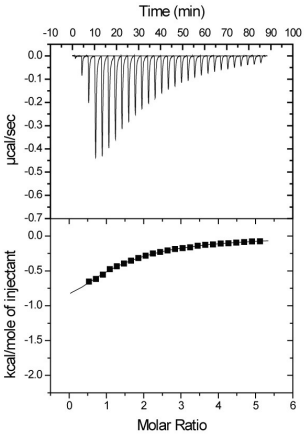

R phosCdc6$^{2-10;\ T9K}$-Cks1

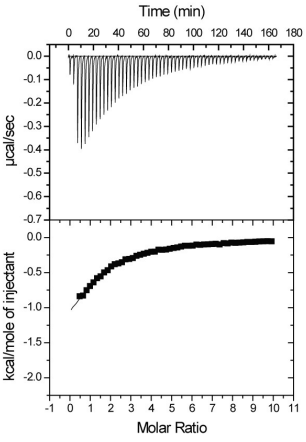

S

phosSic1$^{2-9}$-Cks1

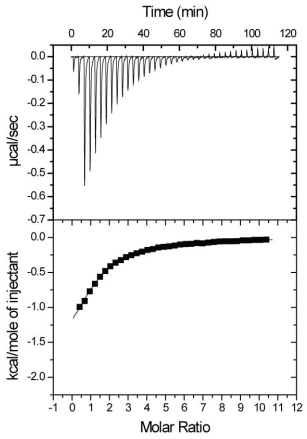

T

phosSic1$^{2-9;\ pT5pS}$-Cks1

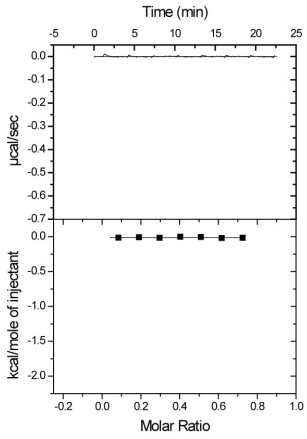

U

phosSic1$^{2-9;\ P6K}$-Cks1

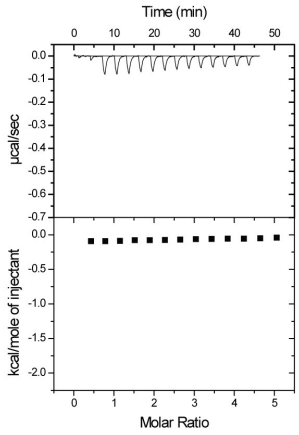

V

phosSic1$^{2-9;\ P3Y}$-Cks1

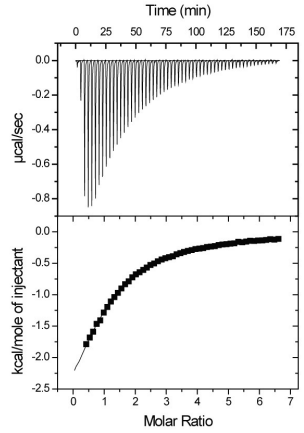

W

phosSic1$^{2-9;\ P3K}$-Cks1

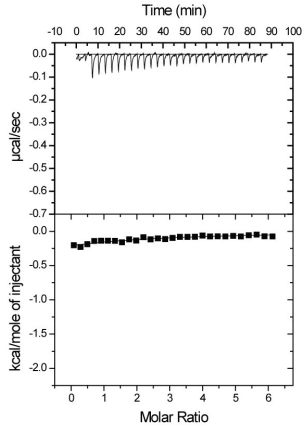

X

phosSic1$^{2-9;\ P7T}$-Cks1

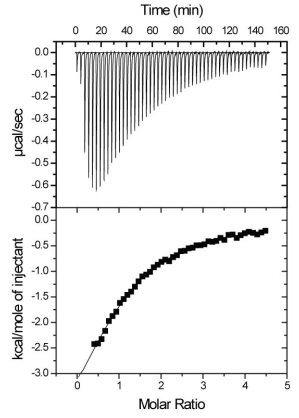

Y

phosSic1$^{2-9;\ P7K}$-Cks1

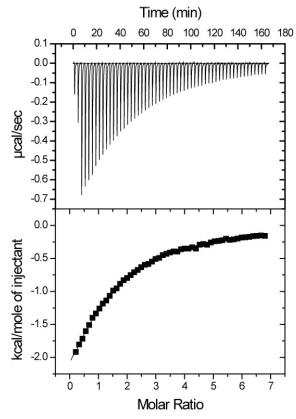

Z

phosCdc6$^{2-10}$-Cks1^{T80D}

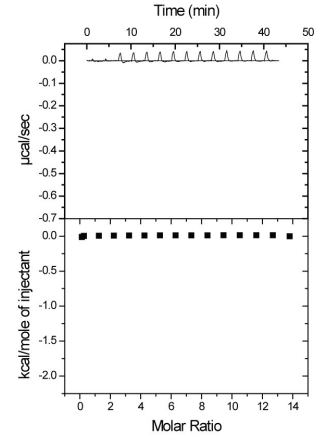

AA

phosCdc6$^{2-10}$-Cks1^{Y30E}

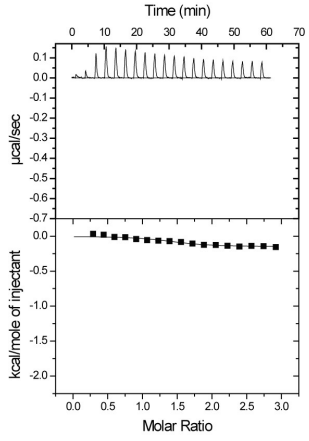

BB phosCdc6$^{2-10}$-Cks1^{L83D}

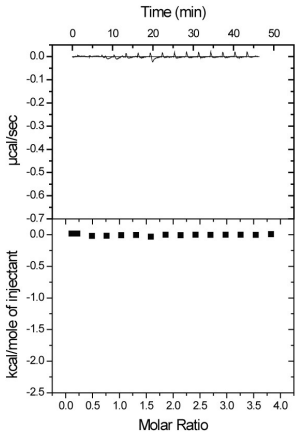

CC phosCdc6$^{2-10}$-Cks1^{R75A}

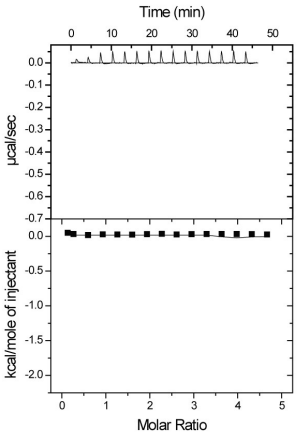

DD phosCdc6$^{2-10}$-Cks1^{R75K}

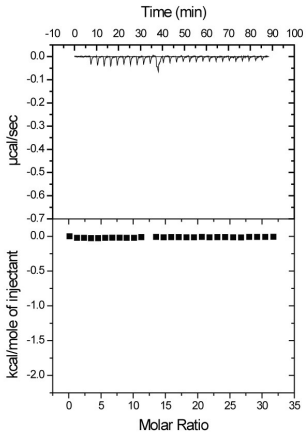

EE phosSwe1$^{41-48}$-Cks1

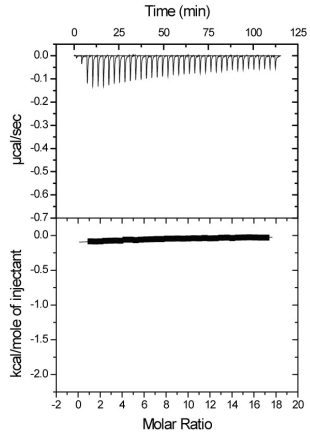

FF phosSwe1$^{117-124}$-Cks1

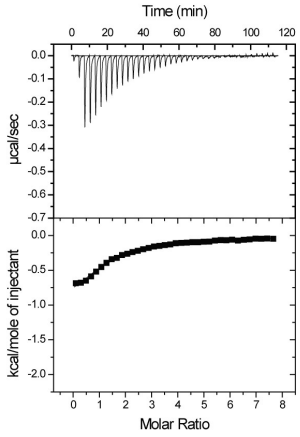

GG phosSwe1$^{192-199}$-Cks1

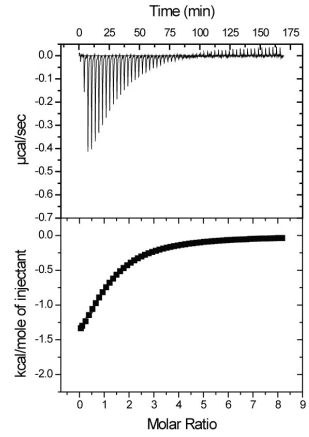

HH phosSwe1$^{369-376}$-Cks1

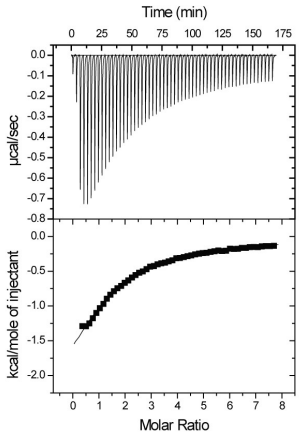

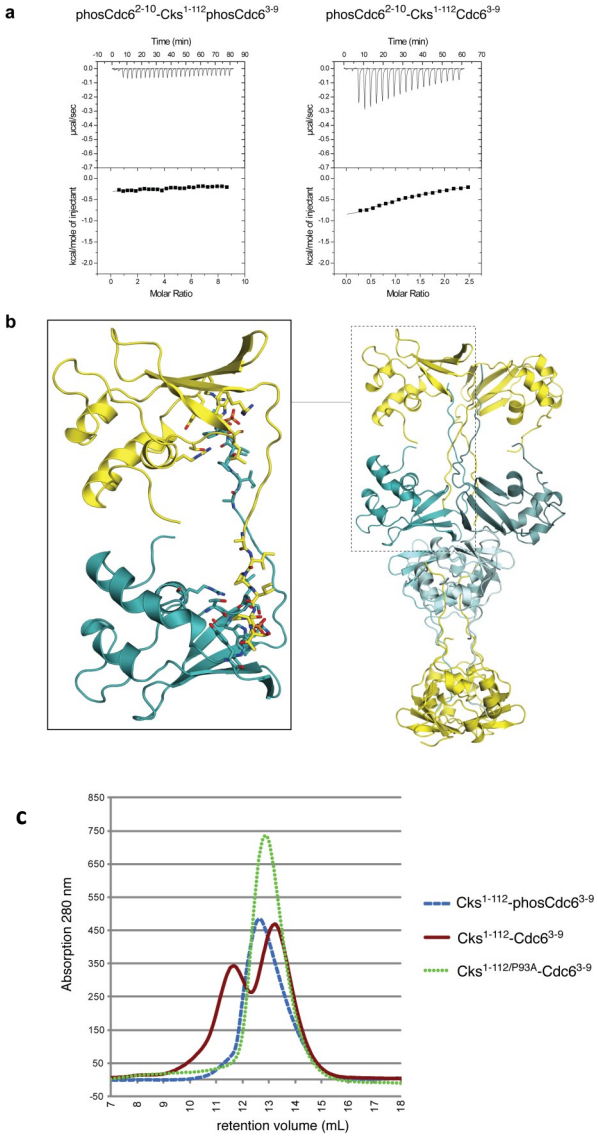

Figure A2. Domain swapping and binding properties of the Cks1-Cdc6 fusion construct. (a) ITC data demonstrate that the Cks11-112-phosCdc63-9 fusion protein binds phosphorylated Cdc6 peptide *in cis* (left), while the unphosphorylated fusion binds the Cdc6 peptide similar to wild-type Cks1 (right). These measurements demonstrate that the phosCdc6 sequence in the fusion can bind Cks1 at the appropriate site and exclude the added peptide. (b) In the crystal structure, the fusion undergoes domain swapping in which the phosCdc6 sequence at the C-terminus of one fusion molecule extends to bind the cationic pocket site on a different Cks1 molecule, related by crystallographic symmetry. Four molecules (cyan) are observed in the asymmetric unit. Unlike in several other Cks crystals33,34, there is no evidence that Cks11-112-phosCdc63-9 forms domainswapped dimers by exchanging strand 4, although the electron density for the loop preceding strand 4 is weak. Instead, dimers are formed between a molecule in the asymmetric unit (cyan) and its crystallographic symmetry mate (yellow) by the swapping of appended phosCdc63-9 sequences. (c) Superdex 75 gel filtration analysis demonstrates that the phosphorylated fusion behaves as a monomer in gel filtration. The unphosphorylated fusion (maroon line) elutes from gel filtration as a double peak, consistent with a monomer-dimer equilibrium in solution and suggesting that the construct undergoes domain swapping similar to Cks1. The phosphorylated Cks11-112-phosCdc63-9 (blue dashes) elutes as a single peak and in the same volume as the monomer-promoting mutant Cks11-112/P93A-Cdc63-9 (green dots)54. We conclude that Cks11-112- phosCdc63-9 fusion protein is a monomer in solution. It is likely that the phosphorylated Cdc6 sequence binds to Cks1 *in cis*, which disrupts the domain-swapped dimerization that occurs through strand 4 in the wild-type protein *in vitro* at high concentrations.

Figure A3. Mutations to Cks that disrupt consensus sequence binding do not disrupt folding or Cdk binding. (a) Circular dichroism spectra of wild-type and mutant Cks1 proteins at a concentration of ~10μM were obtained as previously described54. The spectra demonstrate that the mutations do not disrupt proper folding of Cks1. (b) Binding of Cks1 consensus site mutants to recombinant human Cdk2. The Cks-Cdk interface is highly conserved, and budding yeast Cks1 binds Cdk2 with micromolar affinity54,55. We used Cdk2 to facilitate the *in vitro* binding experiment with recombinant proteins. We mixed 12.5 μM purified His6-Cdk2 with 12.5 μM of the indicated GST-tagged Cks1 protein in a buffer containing 150 mM NaCl, 25mM Tris, and 1 mM DTT (pH 8). The 1 mL binding reaction was mixed with 100 μL GS4B-Sepharose beads and the precipitated beads were washed with binding buffer and eluted with SDS-PAGE sample loading buffer. Input (I), flow-through unbound (U), and bound (B) protein fractions were run on SDS-PAGE and stained with Coomassie Blue. Wild-type and consensus site mutants all bind Cdk2 similarly, which is consistent with the structural observation that the phosphopeptide and Cdk binding interfaces are on opposite faces of Cks (Figure 2.5a).

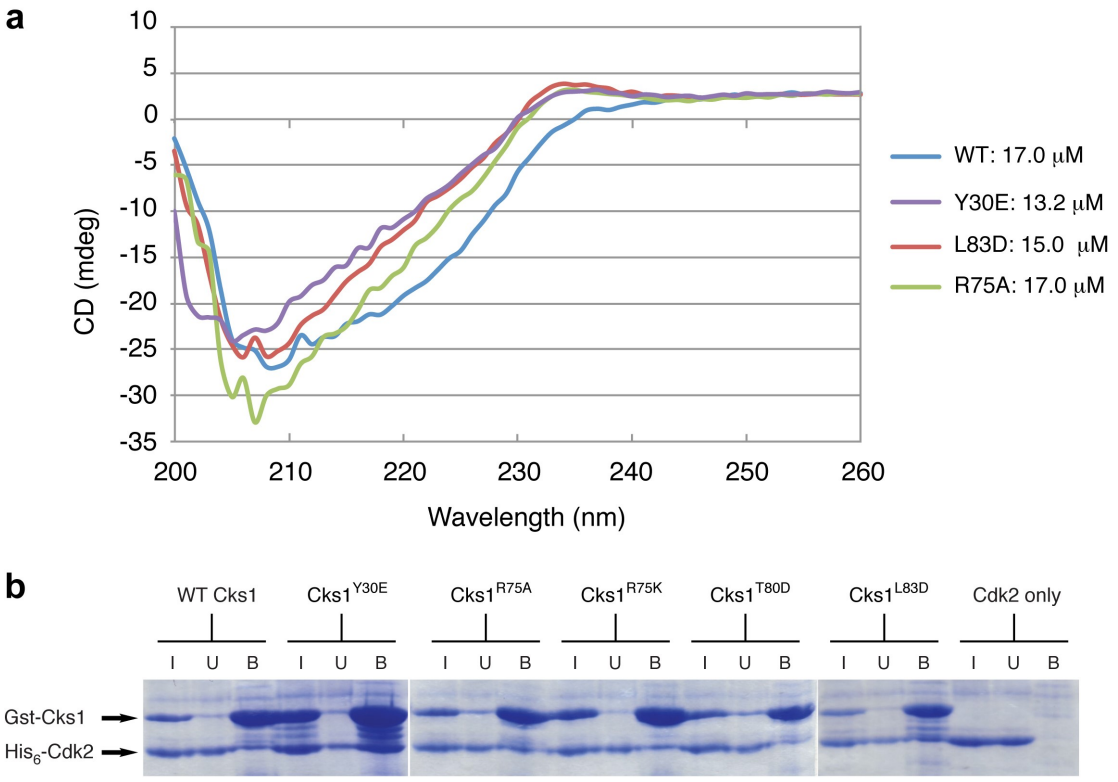

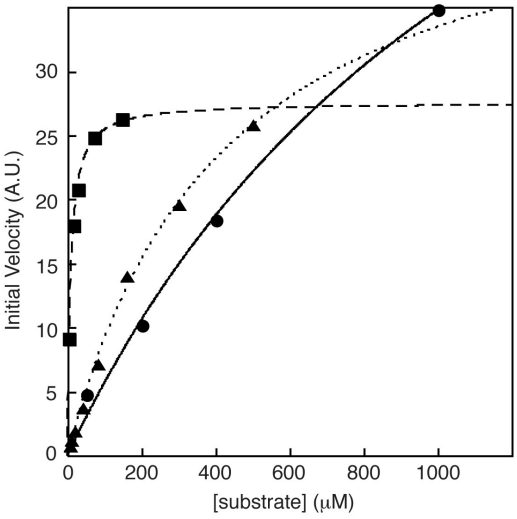

WT Cks1:

Substrate peptide	K_M (μM)	V_{max} (A.U.)	k_{cat} (min^{-1})	k_{cat}/K_M ($\mu M^{-1}min^{-1}$)
● H1	1300 ± 400	80 ± 20	256*	0.2 ± 0.1
▲ Sic1ΔC-T5	420 ± 40	47 ± 3	150 ± 40	0.4 ± 0.1
■ Cdc6 WT	8.3 ± 0.5	27 ± 4	120 ± 30	14 ± 6

Figure A4. Comparison in Cdk kinase reaction of unprimed to primed substrate. Kinase reactions are carried out as described in Figure 4 with wild-type Cks. Both the H1 peptide and Sic1ΔC-T5 construct contain single phosphoacceptor sites. In the Sic1ΔC-T5 construct, all the phosphoacceptor sites except T5 are mutated. The Cdc6 peptide contains phosphorylated T7 and a phosphoacceptor site at T23. The kcat for the reaction with the H1 peptide (marked with *) was previously determined9. Absolute kcat values reported here and in Figure 4 were calculated by comparison of the Vmax value in each experiment to the Vmax determined here for the H1 peptide.

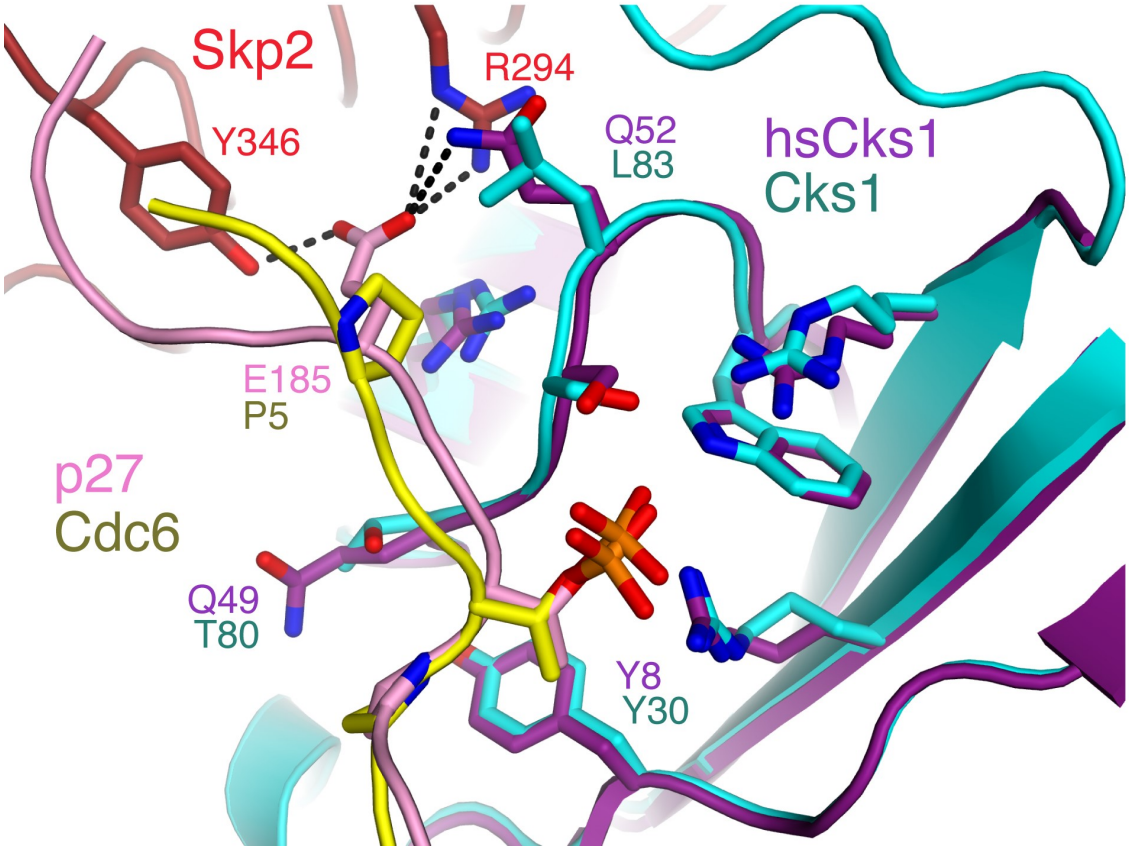

Figure A5. Comparison of the phosCdc6-Cks1 structure determined here with the structure of phosp27-hsCks1-Skp2 (PDB code: 2ast)[36]

Table A1
Putative Cks-binding sequences

90 Cks consensus sites that correspond to validated phosphorylation

ORF Designation	Gene Name	Sequence	Start Residue	End Residue
***YCR088W**	***ABP1***	***VKTP***	***179***	***182***
***YLR131C**	***ACE2***	***LKTP***	***257***	***260***
YLR131C	ACE2	IKTP	529	532
***YJR083C**	***ACF4***	***VTTP***	***47***	***50***
***YPL267W**	***ACM1***	***FITP***	***159***	***162***
***YDR216W**	***ADR1***	***FQTP***	***186***	***189***
YDR216W	ADR1	YGTP	191	194
***YDR216W**	***ADR1***	***FSTP***	***257***	***260***
YBR059C	AKL1	FTTP	264	267
***YOL130W**	***ALR1***	***IHTP***	***141***	***144***
YKR021W	ALY1	YLTP	259	262
YJL084C	ALY2	LSTP	775	778
YOL058W	ARG1	FVTP	316	319
YOL058W	ARG1	YFTP	330	333
YOR058C	ASE1	LATP	33	36
YOR058C	ASE1	LGTP	345	348
YOR058C	ASE1	YKTP	673	676
YKL185W	ASH1	IKTP	6	9
YKL185W	ASH1	PVTP	288	291
YKL185W	ASH1	PSTP	427	430
***YGR097W**	***ASK10***	***VNTP***	***806***	***809***
YMR068W	AVO2	FRTP	217	220
YMR068W	AVO2	VKTP	308	311
YIL140W	AXL2	VATP	21	24
YJL020C	BBC1	PPTP	752	755
YJL095W	BCK1	PQTP	705	708
YJL095W	BCK1	IPTP	763	766
YJL095W	BCK1	PSTP	1081	1084
YER167W	BCK2	FNTP	577	580
YER167W	BCK2	LVTP	509	512
YER167W	BCK2	LSTP	322	325
YER167W	BCK2	ITTP	502	505
YBR200W	BEM1	ISTP	24	27
YER155C	BEM2	PATP	1036	1039
YER155C	BEM2	IETP	1019	1022

YPL115C	BEM3	VMTP	626	629
***YOR198C**	***BFR1**	***LVTP**	***334**	***337**
YFL007W	BLM10	VNTP	1123	1126
YJL060W	BNA3	INTP	204	207
YNL271C	BNI1	FTTP	164	167
YNL271C	BNI1	LQTP	1456	1459
YNL233W	BNI4	LSTP	187	190
YNL233W	BNI4	LKTP	334	337
YNL233W	BNI4	INTP	441	444
YNL233W	BNI4	LSTP	548	551
***YBL085W**	***BOI1**	***VSTP**	***156**	***159**
YBL085W	BOI1	YATP	907	910
YER114C	BOI2	ISTP	974	977
YER114C	BOI2	LPTP	147	150
YER114C	BOI2	IPTP	386	389
YER114C	BOI2	YTTP	899	902
YCL014W	BUD3	VFTP	455	458
YCL014W	BUD3	FYTP	1421	1424
***YCL014W**	***BUD3**	***PNTP**	***1438**	***1441**
YJR092W	BUD4	LKTP	928	931
YJR092W	BUD4	PSTP	981	984
YJR092W	BUD4	VQTP	1106	1109
YLR319C	BUD6	YGTP	10	13
YNL278W	CAF120	VHTP	522	525
YNL278W	CAF120	WPTP	998	1001
***YNL161W**	***CBK1**	***PATP**	***91**	***94**
***YNL161W**	***CBK1**	***INTP**	***107**	***110**
YNL161W	CBK1	VGTP	572	575
YFR028C	CDC14	VLTP	180	183
***YMR001C**	***CDC5**	***VHTP**	***21**	***24**
***YJL194W**	***CDC6**	***PITP**	***5**	***8**
***YJL194W**	***CDC6**	***PATP**	***21**	***24**
***YJL194W**	***CDC6**	***LSTP**	***133**	***136**
***YJL194W**	***CDC6**	***PLTP**	***366**	***369**
***YGL003C**	***CDH1**	***VSTP**	***155**	***158**
***YGL003C**	***CDH1**	***PVTP**	***174**	***177**
YBR038W	CHS2	VFTP	894	897
YNL298W	CLA4	VGTP	729	732
YAL040C	CLN3	PLTP	515	518
YFR046C	CNN1	IRTP	19	22

YDR223W	CRF1	ILTP	216	219
YDR223W	CRF1	LPTP	354	357
YDR223W	CRF1	INTP	412	415
YPR030W	CSR2	VRTP	617	620
YPR030W	CSR2	VDTP	918	921
YPR030W	CSR2	IFTP	1073	1076
***YOR042W**	***CUE5**	***VVTP**	***68**	***71**
***YOR042W**	***CUE5**	***IDTP**	***362**	***365**
YIR023W	DAL81	YATP	606	609
YIR023W	DAL81	PQTP	639	642
YGR092W	DBF2	PFTP	491	494
YPL194W	DDC1	YLTP	442	445
YHR164C	DNA2	PGTP	2	5
***YDR093W**	***DNF2**	***ISTP**	***68**	***71**
YDR093W	DNF2	PCTP	691	694
YBL101C	ECM21	IRTP	564	567
YBL101C	ECM21	LNTP	820	823
YBL101C	ECM21	IDTP	867	870
***YBL101C**	***ECM21**	***LSTP**	***1026**	***1029**
YBL047C	EDE1	FRTP	6	9
YBL047C	EDE1	LQTP	1151	1154
***YBL047C**	***EDE1**	***VATP**	***1305**	***1308**
YNL230C	ELA1	PITP	267	270
YKL048C	ELM1	PITP	32	35
YKL048C	ELM1	IFTP	283	286
YKL048C	ELM1	VGTP	308	311
YKL048C	ELM1	IPTP	549	552
YMR219W	ESC1	LTTP	17	20
***YFR019W**	***FAB1**	***ISTP**	***390**	***393**
YFR019W	FAB1	LITP	1362	1365
***YFR019W**	**FAB1**	**LNTP**	**1951**	**1954**
YFR019W	FAB1	VVTP	2248	2251
***YJL157C**	***FAR1**	***IHTP**	***13**	***16**
YJL157C	FAR1	FRTP	322	325
YER032W	FIR1	PVTP	4	7
YER032W	FIR1	PLTP	212	215
YER032W	FIR1	YLTP	220	223
YER032W	FIR1	LSTP	358	361
YNL068C	FKH2	IKTP	549	552
YNR047W	FPK1	LQTP	153	156

***YNR047W**	***FPK1**	***PSTP**	***199**	***202**
YNR047W	FPK1	LSTP	283	286
YPL141C	FRK1	YTTP	551	554
YAL035W	FUN12	IDTP	475	478
YAL035W	FUN12	LLTP	678	681
YAL035W	FUN12	VGTP	893	896
***YCL027W**	***FUS1**	***ILTP**	***176**	***179**
***YCL027W**	***FUS1**	***LKTP**	***279**	***282**
YCL027W	FUS1	IPTP	390	393
***YCL027W**	***FUS1**	***PLTP**	***422**	***425**
YOR178C	GAC1	ISTP	575	578
YOL051W	GAL11	LLTP	207	210
YPL248C	GAL4	PLTP	758	761
YDL226C	GCS1	WATP	36	39
YDR309C	GIC2	ISTP	134	137
YDR309C	GIC2	LETP	318	321
YDR309C	GIC2	IATP	346	349
YDR507C	GIN4	YLTP	310	313
***YDR507C**	***GIN4**	***LTTP**	***433**	***436**
YDR507C	GIN4	IPTP	845	848
YER054C	GIP2	PTTP	196	199
YDR096W	GIS1	VLTP	453	456
YDR096W	GIS1	FGTP	470	473
***YLR258W**	***GSY2**	***YMTP**	***666**	***669**
***YMR192W**	***GYL1**	***PRTP**	***15**	***18**
YOR070C	GYP1	FGTP	179	182
YOR070C	GYP1	LVTP	383	386
YOR070C	GYP1	PVTP	526	529
***YOR070C**	***GYP1**	***FVTP**	***537**	***540**
YJL165C	HAL5	LSTP	234	237
YCR065W	HCM1	LKTP	426	429
YCR065W	HCM1	ISTP	445	448
YCR065W	HCM1	WQTP	458	461
YCR065W	HCM1	IETP	477	480
YCR065W	HCM1	ITTP	484	487
YOR227W	HER1	ISTP	213	216
YKL101W	HSL1	VLTP	1185	1188
YHR094C	HXT1	FFTP	481	484
YJL146W	IDS2	IGTP	41	44
YDR123C	INO2	VRTP	263	266

***YOR109W**	***INP53**	***PLTP**	***1103**	***1106**
YOR109W	INP53	ILTP	1024	1027
YPL242C	IQG1	LITP	297	300
YPR141C	KAR3	PRTP	5	8
***YPR141C**	***KAR3**	***LSTP**	***17**	***20**
YPL269W	KAR9	FQTP	596	599
YPL269W	KAR9	ITTP	603	606
YPL269W	KAR9	PPTP	623	626
YHR158C	KEL1	LSTP	33	36
***YHR158C**	***KEL1**	***LATP**	***475**	***478**
YHR158C	KEL1	ILTP	547	550
YHR158C	KEL1	FDTP	570	573
YHR158C	KEL1	IKTP	624	627
YGR238C	KEL2	IVTP	39	42
YGR238C	KEL2	ILTP	453	456
YHR102W	KIC1	LPTP	600	603
YHR102W	KIC1	LPTP	832	835
***YHR102W**	***KIC1**	***ISTP**	***1071**	***1074**
YLR096W	KIN2	PLTP	394	397
YLR096W	KIN2	PLTP	1029	1032
YOR233W	KIN4	YITP	281	284
YPL155C	KIP2	ISTP	273	276
YGL216W	KIP3	PETP	252	255
YGL216W	KIP3	PSTP	774	777
YCL051W	LRE1	LSTP	20	23
YCL051W	LRE1	LQTP	108	111
YCL051W	LRE1	PATP	308	311
YAL024C	LTE1	YPTP	10	13
YAL024C	LTE1	FITP	63	66
YAL024C	LTE1	PPTP	315	318
YAL024C	LTE1	PFTP	1130	1133
***YDL182W**	***LYS20**	***VSTP**	***394**	***397**
***YDL131W**	***LYS21**	***LSTP**	***408**	***411**
YJL013C	MAD3	FETP	273	276
YJL013C	MAD3	PMTP	455	458
YEL032W	MCM3	IPTP	225	228
***YEL032W**	***MCM3**	***VGTP**	***866**	***869**
YGL197W	MDS3	PNTP	656	659
YGL197W	MDS3	YSTP	674	677
YGL197W	MDS3	FGTP	852	855

YGL197W	MDS3	IQTP	967	970
YGL197W	MDS3	LLTP	1003	1006
YMR036C	MIH1	LDTP	498	501
YNL074C	MLF3	VRTP	65	68
YLR035C	MLH2	IPTP	387	390
YLR035C	MLH2	LFTP	689	692
***YLL061W**	***MMP1**	***LSTP**	***19**	***22**
YLR190W	MMR1	PATP	197	200
YBR098W	MMS4	LSTP	300	303
***YIL106W**	***MOB1**	***LTTP**	***83**	***86**
YFL034C-B	MOB2	YVTP	147	150
YGL124C	MON1	WVTP	597	600
YPL082C	MOT1	ILTP	472	475
YPL082C	MOT1	LNTP	643	646
YPL082C	MOT1	FSTP	754	757
YGL075C	MPS2	ISTP	139	142
YOR066W	MSA1	LSTP	82	85
YOR066W	MSA1	ISTP	97	100
YOR066W	MSA1	PSTP	278	281
YOR066W	MSA1	FNTP	404	407
YOR066W	MSA1	PSTP	542	545
YKR077W	MSA2	YTTP	3	6
YKR077W	MSA2	PRTP	164	167
YOR188W	MSB1	LPTP	8	11
YGR014W	MSB2	LLTP	910	913
YGR014W	MSB2	LNTP	1039	1042
YDR097C	MSH6	PATP	3	6
YDR097C	MSH6	VLTP	1014	1017
YKL062W	MSN4	VATP	140	143
YAR033W	MST28	WHTP	143	146
YPL070W	MUK1	LFTP	5	8
YPL070W	MUK1	IVTP	460	463
YKL129C	MYO3	IKTP	701	704
YKL129C	MYO3	INTP	894	897
YKL129C	MYO3	YMTP	1176	1179
YOL070C	NBA1	LPTP	308	311
YOL070C	NBA1	PSTP	355	358
YOR372C	NDD1	FPTP	55	58
YOR372C	NDD1	VGTP	275	278
YOR372C	NDD1	IKTP	330	333

YJL076W	NET1	VSTP	210	213
YJL076W	NET1	VTTP	355	358
YJL076W	NET1	VNTP	1015	1018
YOR056C	NOB1	YTTP	35	38
YOR056C	NOB1	WITP	223	226
***YPR072W**	***NOT5**	***LGTP**	***304**	***307**
YML059C	NTE1	YYTP	1348	1351
YDR001C	NTH1	IDTP	215	218
YIL115C	NUP159	FGTP	555	558
YIL115C	NUP159	FGTP	581	584
***YIL115C**	***NUP159**	***PETP**	***801**	***804**
YPR091C	NVJ2	IKTP	343	346
YPR091C	NVJ2	YPTP	495	498
YHL029C	OCA5	IATP	148	151
YBR060C	ORC2	PKTP	68	71
YBR060C	ORC2	PATP	172	175
***YHR118C**	***ORC6**	***FGTP**	***144**	***147**
YIL050W	PCL7	LLTP	143	146
YDR113C	PDS1	PQTP	25	28
***YOR104W**	***PIN2**	***VKTP**	***139**	***142**
YOR104W	PIN2	YNTP	251	254
YBL051C	PIN4	FTTP	133	136
YBL105C	PKC1	LLTP	956	959
YOL100W	PKH2	PYTP	635	638
YOL100W	PKH2	PMTP	643	646
YOL100W	PKH2	IQTP	924	927
YDR501W	PLM2	YPTP	46	49
YDR501W	PLM2	PSTP	319	322
YIL122W	POG1	IHTP	342	345
YNL102W	POL1	PGTP	311	314
YNL102W	POL1	YQTP	452	455
***YNL102W**	***POL1**	***LFTP**	***1320**	***1323**
***YBL035C**	***POL12**	***PKTP**	***109**	***112**
YBL035C	POL12	FQTP	183	186
YBL035C	POL12	LFTP	468	471
YMR129W	POM152	IKTP	780	783
***YLR018C**	***POM34**	***LETP**	***219**	***222**
***YLR018C**	***POM34**	***PHTP**	***271**	***274**
***YIL114C**	***POR2**	***FLTP**	***101**	***104**
YML016C	PPZ1	PSTP	65	68

YML016C	PPZ1	LTTP	104	107
***YML016C**	***PPZ1**	***YSTP**	***259**	***262**
YDR436W	PPZ2	PITP	91	94
YDR436W	PPZ2	YSTP	269	272
YKL116C	PRR1	PKTP	11	14
YKL116C	PRR1	LPTP	72	75
YKL116C	PRR1	IKTP	294	297
YML017W	PSP2	WTTP	188	191
***YBL046W**	***PSY4**	***LTTP**	***345**	***348**
YJR059W	PTK2	PYTP	435	438
***YJR059W**	***PTK2**	***PTTP**	***728**	***731**
YKR090W	PXL1	VETP	361	364
YDR217C	RAD9	FQTP	153	156
YDR217C	RAD9	IVTP	216	219
YDR217C	RAD9	FETP	472	475
YJR033C	RAV1	LNTP	495	498
YDL189W	RBS1	FGTP	357	360
YLR248W	RCK2	IFTP	348	351
YDR195W	REF2	VATP	332	335
YOR127W	RGA1	LPTP	147	150
YOR127W	RGA1	LDTP	468	471
YOR127W	RGA1	PATP	530	533
YOR127W	RGA1	YRTP	539	542
YDR379W	RGA2	VNTP	318	321
YDR379W	RGA2	FRTP	559	562
YPR115W	RGC1	PATP	19	22
YPR115W	RGC1	YITP	759	762
***YPR115W**	***RGC1**	***VNTP**	***815**	***818**
YPR115W	RGC1	IRTP	845	848
YDR137W	RGP1	ITTP	524	527
YKL038W	RGT1	PSTP	140	143
YKL038W	RGT1	VTTP	455	458
YBR275C	RIF1	LRTP	598	601
YBR275C	RIF1	LITP	648	651
YFL033C	RIM15	LPTP	553	556
YFL033C	RIM15	FLTP	745	748
YFL033C	RIM15	LSTP	984	987
YFL033C	RIM15	FGTP	1148	1151
YFL033C	RIM15	FLTP	1219	1222
YFL033C	RIM15	YITP	1380	1383

YFL033C	RIM15	VSTP	1476	1479
YLR371W	ROM2	FSTP	1078	1081
YER169W	RPH1	FTTP	178	181
YER169W	RPH1	FSTP	608	611
YER169W	RPH1	IKTP	631	634
YIL153W	RRD1	FSTP	13	16
YOR001W	RRP6	PLTP	408	411
YLR357W	RSC2	WKTP	436	439
***YOR014W**	***RTS1**	***LPTP**	***240**	***243**
***YOR014W**	***RTS1**	***IKTP**	***255**	***258**
YDR159W	SAC3	LLTP	634	637
YDR159W	SAC3	FRTP	842	845
YDR159W	SAC3	FKTP	1165	1168
YDR159W	SAC3	VSTP	1207	1210
YDR159W	SAC3	PVTP	1265	1268
YDR389W	SAC7	YNTP	71	74
YER129W	SAK1	VGTP	323	326
YGL056C	SDS23	LSTP	14	17
***YGL056C**	***SDS23**	***PSTP**	***403**	***406**
YBR214W	SDS24	LSTP	31	34
YPL085W	SEC16	IVTP	579	582
YPL085W	SEC16	LGTP	593	596
YPL085W	SEC16	VNTP	826	829
YER008C	SEC3	VSTP	296	299
YDL195W	SEC31	PLTP	150	153
YDL195W	SEC31	LPTP	775	778
YDL195W	SEC31	LSTP	947	950
***YDL195W**	***SEC31**	***VATP**	***1048**	***1051**
YDL195W	SEC31	PLTP	1186	1189
***YMR086W**	***SEG1**	***VVTP**	***576**	***579**
***YMR086W**	***SEG1**	***LGTP**	***673**	***676**
YHR098C	SFB3	YTTP	54	57
YOR315W	SFG1	LRTP	12	15
YOR315W	SFG1	PSTP	26	29
YLL003W	SFI1	LKTP	814	817
***YLR079W**	***SIC1**	***PSTP**	***3**	***6**
***YLR079W**	***SIC1**	***PVTP**	***43**	***46**
***YLR079W**	***SIC1**	***PGTP**	***171**	***174**
YOL004W	SIN3	IDTP	257	260
***YOL004W**	***SIN3**	***VTTP**	***302**	***305**

YOL004W	SIN3	WLTP	966	969
YDR422C	SIP1	PSTP	615	618
YNL257C	SIP3	PTTP	498	501
YDL042C	SIR2	PETP	107	110
YDR227W	SIR4	PVTP	20	23
YDR227W	SIR4	VKTP	37	40
YKR072C	SIS2	PATP	334	337
YEL065W	SIT1	PLTP	343	346
YEL065W	SIT1	WGTP	542	545
YDR409W	SIZ1	LSTP	694	697
YLR187W	SKG3	PSTP	26	29
YLR187W	SKG3	ISTP	53	56
YLR187W	SKG3	FTTP	551	554
YHR149C	SKG6	VPTP	536	539
YHR149C	SKG6	LPTP	556	559
***YNL167C**	***SKO1**	***ILTP**	***111**	***114**
YNL167C	SKO1	PLTP	280	283
YNL167C	SKO1	VSTP	495	498
YBL007C	SLA1	PQTP	16	19
YNL243W	SLA2	PLTP	601	604
YGL113W	SLD3	IHTP	172	175
YGL113W	SLD3	LKTP	551	554
YDR515W	SLF1	PITP	81	84
YDR515W	SLF1	LQTP	257	260
YOR195W	SLK19	PTTP	5	8
YNL047C	SLM2	LGTP	321	324
YNL047C	SLM2	VLTP	468	471
YNL047C	SLM2	FKTP	477	480
YNL047C	SLM2	FSTP	485	488
YLR086W	SMC4	ISTP	755	758
YDR006C	SOK1	VITP	110	113
YDR006C	SOK1	YPTP	636	639
YLL021W	SPA2	PMTP	550	553
YGL093W	SPC105	VATP	153	156
YGL093W	SPC105	VTTP	354	357
***YKL042W**	***SPC42**	***FATP**	***355**	***358**
***YML034W**	***SRC1**	***VKTP**	***239**	***242**
YML034W	SRC1	ITTP	352	355
YML034W	SRC1	IETP	392	395
YKR091W	SRL3	LKTP	3	6

YKR091W	SRL3	LATP	38	41
YKR091W	SRL3	PITP	82	85
YJL092W	SRS2	VITP	602	605
YNR031C	SSK2	LTTP	170	173
YNR031C	SSK2	VLTP	967	970
YDR443C	SSN2	VPTP	74	77
YDR443C	SSN2	LITP	208	211
YDR443C	SSN2	YLTP	258	261
YDR443C	SSN2	YRTP	316	319
YDR443C	SSN2	LNTP	397	400
YDR443C	SSN2	VETP	599	602
YDR443C	SSN2	FITP	833	836
***YNL309W**	***STB1***	***PNTP***	***97***	***100***
YNL309W	STB1	PSTP	123	126
YNL309W	STB1	FMTP	150	153
YNL309W	STB1	PTTP	216	219
YNL309W	STB1	PTTP	310	313
YNL309W	STB1	LRTP	325	328
***YFL026W**	***STE2***	***LPTP***	***380***	***383***
YHL007C	STE20	VSTP	205	208
YHL007C	STE20	ISTP	337	340
***YHL007C**	***STE20***	***VSTP***	***421***	***424***
***YHL007C**	***STE20***	***PTTP***	***510***	***513***
***YHL007C**	***STE20***	***VTTP***	***571***	***574***
***YHL007C**	***STE20***	***VGTP***	***775***	***778***
YDR103W	STE5	VFTP	454	457
YDL048C	STP4	IDTP	29	32
YLR045C	STU2	LKTP	403	406
YLR045C	STU2	VFTP	416	419
YLR045C	STU2	LATP	643	646
YDR310C	SUM1	PVTP	316	319
***YJL187C**	***SWE1***	***VTTP***	***119***	***122***
***YJL187C**	***SWE1***	***PETP***	***194***	***197***
***YJL187C**	***SWE1***	***ISTP***	***371***	***374***
YER111C	SWI4	FQTP	213	216
YER111C	SWI4	LITP	584	587
YER111C	SWI4	FNTP	685	688
YDR146C	SWI5	FITP	318	321
YML072C	TCB3	LYTP	1116	1119
YMR291W	TDA1	FNTP	511	514

***YMR291W**	***TDA1**	***LLTP**	***536**	***539**
YHR159W	TDA11	LMTP	64	67
YHR159W	TDA11	PTTP	112	115
***YHR159W**	***TDA11**	***LNTP**	***234**	***237**
YKR089C	TGL4	LKTP	639	642
YKR089C	TGL4	IETP	808	811
YOR081C	TGL5	PSTP	344	347
YGL049C	TIF4632	PSTP	142	145
***YGL049C**	***TIF4632**	***VKTP**	***299**	***302**
YGL049C	TIF4632	FVTP	763	766
YNL088W	TOP2	FITP	559	562
YGR221C	TOS2	LPTP	440	443
YGR221C	TOS2	FCTP	506	509
YLR183C	TOS4	YPTP	51	54
YMR261C	TPS3	PYTP	11	14
YMR261C	TPS3	VITP	197	200
***YER093C**	***TSC11**	***LLTP**	***26**	***29**
YER093C	TSC11	LTTP	232	235
YML100W	TSL1	IVTP	203	206
YML100W	TSL1	IQTP	1007	1010
YLR425W	TUS1	LLTP	527	530
YLR425W	TUS1	FSTP	800	803
YLR425W	TUS1	ILTP	1062	1065
YGR184C	UBR1	VETP	490	493
***YPL020C**	***ULP1**	***VGTP**	***177**	***180**
YPL020C	ULP1	IFTP	504	507
YIL031W	ULP2	FETP	422	425
YML029W	USA1	PHTP	67	70
YIL135C	VHS2	VQTP	115	118
YOR054C	VHS3	LDTP	47	50
YOR054C	VHS3	FSTP	156	159
YOR054C	VHS3	LHTP	212	215
YLR410W	VIP1	VPTP	290	293
YHL035C	VMR1	FVTP	579	582
YHL035C	VMR1	LKTP	616	619
YHL035C	VMR1	VITP	1136	1139
***YNL321W**	***VNX1**	***VLTP**	***24**	***27**
YLL040C	VPS13	WDTP	708	711
YLL040C	VPS13	VLTP	1020	1023
YLL040C	VPS13	VNTP	2165	2168

YLR337C	VRP1	PPTP	242	245
YLR337C	VRP1	LPTP	581	584
YML076C	WAR1	VLTP	405	408
YOR083W	WHI5	LRTP	3	6
YOR083W	WHI5	LSTP	45	48
***YOR083W**	***WHI5**	***FGTP**	***55**	***58**
YOR083W	WHI5	PTTP	141	144
YOR083W	WHI5	VQTP	213	216
YHL028W	WSC4	LHTP	471	474
YHL028W	WSC4	FSTP	482	485
YML027W	YOX1	LLTP	110	113
YML027W	YOX1	ILTP	130	133
YGR296W	YRF1-3	PNTP	379	382
YNL339C	YRF1-6	PNTP	379	382
YDR326C	YSP2	IITP	1312	1315
***YGR270W**	***YTA7**	***PETP**	***210**	***213**
YGR270W	YTA7	ISTP	1101	1104
YGR270W	YTA7	ILTP	1321	1324
YNR039C	ZRG17	FQTP	21	24
YER033C	ZRG8	PSTP	44	47
YER033C	ZRG8	FKTP	206	209
YER033C	ZRG8	LQTP	764	767
YER033C	ZRG8	VITP	771	774
YER033C	ZRG8	LRTP	802	805
YBL005W-A		PTTP	55	58
YBL005W-A		LNTP	141	144
YBR138C		PLTP	54	57
YCL019W		LHTP	513	516
YFL042C		IRTP	508	511
YGL235W		LPTP	88	91
YGR035C		LLTP	2	5
YGR237C		LGTP	85	88
YLL032C		YFTP	133	136
YLL032C		VITP	364	367
YLR049C		LFTP	103	106
YLR278C		PPTP	94	97
YMR124W		LSTP	491	494
YMR196W		PRTP	951	954
YPL150W		LPTP	805	808
YEL043W		IKTP	36	39

YIR007W	PNTP	746	749
YJR054W	VNTP	390	393
YJR054W	IYTP	468	471
YOL036W	IITP	287	290
YOL036W	LPTP	391	394
YOL036W	VSTP	507	510
YOL036W	PTTP	571	574

Table A2. Data collection and refinement statistics.	SpeedyBox-Cdk2
Resolution range	65.01 - 2.7 (2.797 - 2.7)
Space group	P 41 21 2
Unit cell	120.91 120.91 77.1099 90 90 90
Total reflections	32412 (3144)
Unique reflections	16212 (1573)
Multiplicity	2.0 (2.0)
Completeness (%)	1.00 (1.00)
Mean I/sigma(I)	13.32 (2.05)
Wilson B-factor	63.92
R-merge	0.03113 (0.3251)
R-meas	0.04403 (0.4598)
CC1/2	0.999 (0.757)
CC*	1 (0.928)
Reflections used in refinement	16209 (1572)
Reflections used for R-free	1622 (158)
R-work	0.2158 (0.3175)
R-free	0.2711 (0.3562)
CC(work)	0.951 (0.769)
CC(free)	0.912 (0.698)
Number of non-hydrogen atoms	3569
macromolecules	3548
Protein residues	430
RMS(bonds)	0.008
RMS(angles)	1.01
Ramachandran favored (%)	93
Ramachandran allowed (%)	6
Ramachandran outliers (%)	0.93
Rotamer outliers (%)	1.6
Clashscore	13.63
Average B-factor	74.44
macromolecules	74.54
solvent	57.49
Number of TLS groups	15
Statistics for the highest-resolution shell are shown in parentheses.	